Sensors & Diagnostics

CRITICAL REVIEW

View Article Online
View Journal | View Issue

Cite this: *Sens. Diagn.*, 2024, **3**, 1769

A review on $Ti_3C_2T_x$ based nanocomposites for the electrochemical sensing of clinically relevant biomarkers

Anjali Sugunan, Anusree V. Rethnakumaran and Mini Mol Menamparambath *

Received 23rd May 2024,
Accepted 26th September 2024

DOI: 10.1039/d4sd00171k

rsc.li/sensors

Reckoning the significance of next-generation biosensors and point-of-care sensors, scientists are interested in developing superior nanomaterials with advantageous characteristics that can serve as electrode modifiers in the development of functional devices. MXenes are a broad class of two-dimensional metal carbides and nitrides characterized by their exceptional hydrophilicity, high specific surface area, and high conductivity. MXenes and their derived nanocomposites are presently gaining importance as electrode materials for the electrochemical detection of various biomarkers. This review assesses and summarises current notable accomplishments in the concepts, fabrication, and diverse applications of MXene-based nanocomposites for electrochemical monitoring of a variety of clinically relevant biomarkers. Furthermore, an outline of the existing impediments linked to technological advancement is included, accompanied by proposals for further investigation into the issues.

1. Introduction

Over the last decade, the research community has witnessed impressive growth in the field of electrochemical sensing aiming towards point-of-care diagnostics (POC) as a direct consequence of significant advancements in new concepts and knowledge in electrochemistry, microelectronics, and material processing.[1] Withal, the efficient use of functional nanomaterials in different electroanalytical tests in recent years has resulted in the quick, sensitive, and selective detection and monitoring of a wide range of biomarkers in bodily fluids.[2–4]

Biomarkers are a class of cellular, biochemical, or molecular alterations observable in biological media, offering enormous potential for use in various clinical situations, including early disease detection, risk assessment, prognosis, prediction of patients' response to therapeutic intervention, and disease progression or recurrence monitoring.[4] Moreover, biomarkers are ideal molecules to reflect the entire spectrum of disease, from early manifestations to the terminal stages of fatal diseases such as psychological/psychiatric disorders, cancerous growth, and circulatory system disorders.[4] Biomarkers can be broadly classified into two categories: exposure biomarkers, which are utilised for risk prediction, and disease biomarkers, which are employed for screening, diagnosis, and monitoring of disease developments.[5] Disease biomarkers are valuable for early detection or enable the determination of the desired outcome at a more rudimentary stage of the disease. The tests of blood, urine, and cerebrospinal fluids give essential information for clinical diagnosis. Conventional experimental and data analytical techniques such as mass spectrometry, nuclear magnetic resonance (NMR), spectrophotometric methods, and chromatography require high-end and costly instruments and an expert technician for operation and result interpretation.[6]

Highly sensitive and selective electrochemical sensors are low-cost alternatives to these conventional techniques because they eliminate the need for intricate procedures, expensive reagents, and professional expertise. Likewise, electrochemical sensors are appealing due to the possibility of device miniaturisation and the ability to develop disposable, flexible, wearable, or implantable devices.[7] Electrochemical sensors, thereby, have the potential to play a crucial role in health monitoring, particularly in POC diagnostics, due to their easy use, low cost, excellent sensitivity and selectivity, portability, and user-friendliness.[2,8,9] Over the years, the advancements in microfabrication, nanotechnology, and the need for modern medical diagnosis paved the way for research on sensitive and reliable electrochemical sensors rooted in innovative functional materials.

Various functional materials employed in fabricating electrodes have evolved over the years to optimise the analytical performance of electrochemical sensors to increase

Department of Chemistry, National Institute of Technology Calicut, Calicut-673601, Kerala, India. E-mail: neeharabindu@gmail.com, minimol@nitc.ac.in

sensitivity and selectivity for analysing biomarkers from complex biological fluids.[10–12] The susceptibility of the sensor depends on the efficient transport of electrons at the electrode–electrolyte interface and, consequently, the high current density in response to the analyte concentrations. Further, the sensitivity of the electrode is enhanced with the application of potential biological molecules, electrochemically active organic/inorganic materials, and their versatile processing techniques.[10] The massive proliferation of potential research in nanomaterials and their composites has opened greater horizons in nanomaterial-based electrochemical sensors. Owing to the high surface area and electrocatalytic activities, the nanostructure-modified electrodes have several advantages over standard macro electrodes, including improved mass transport, lower detection limits, and higher signal-to-noise ratios. Hence, biomarker sensing research encompasses active research on transition metal-based nanostructures, oxides, carbon-based nanomaterials, conductive polymers, metal–organic frameworks (MOFs), *etc.*[13] Two-dimensional nanomaterials (2DNMs) are chosen over 0D and 1D nanomaterials as they have a superior surface-to-volume ratio, which increases their chemical reactivity and ensures impactful interaction between the stimulus and material. On account of the tunable conductivity, band gap, high mechanical flexibility, and excellent electrocatalytic activities, 2DNMs can replace other sensing materials in various electroanalytical devices.[14] MXenes are innovative additions to the rapidly expanding family of 2D materials with beneficial and customizable physicochemical properties, such as regular metal atomic layers, high electrical conductivity, hydrophilicity, ease of synthesis and functionalization, excellent mechanical strength, and biocompatibility.[15] The above-mentioned fundamental features of MXenes fulfil the requirements for an alternative sensor material; hence, MXene has received much interest in the electrochemical monitoring of biomarkers.

In this review, we focus on numerous $Ti_3C_2T_x$ MXene-based composites recently reported in the electrochemical sensor domain for monitoring biomarkers of clinical importance that are otherwise difficult to detect at an early stage using conventional techniques. The synthesis methods of MXene-based composites are of great importance since they can directly or indirectly influence their final characteristics and applications. Researchers believe that the synergistic effects of high conductivity, large specific area nanosheet structure, and varied surface chemistry are responsible for the significant performance of MXene nanocomposites. MXene-based nanocomposites have shown intriguing promise and are attracting considerable interest for the electrochemical detection of neurotransmitters, small biomolecules, *etc.* Furthermore, the future directions and perspectives of these hybrid composites for the possibility of upcoming point-of-care sensor applications, a rapidly growing field in the era of MXene-based composites, are discussed.

2. Exploration of MXenes as electrochemical sensors

MXene, discovered in 2011, is a revolutionary 2D conductive material of early transition metal carbides, nitrides, or carbonitrides.[16] MXenes are 2D flakes formed with $n + 1$ ($n = 1$ to 3) layers of early transition metals (such as Sc, Ti, Zr, Hf, V, Nb, Ta, Cr, Mo, *etc.*) interleaved with n layers of carbon or nitrogen, with a typical formula of $M_{n+1}X_nT_x$, where M denotes the early transition metal, X is C and/or N, and T_x represents the surface terminations, such as O, OH, F, and/or Cl.[17] The term "MXene" was coined to refer to its parent MAX phases and to describe its dimensional similarities to graphene.[18] MXene is a rapidly developing 2D material family, with over thirty stoichiometric compositions synthesised to date and over one hundred MXenes predicted theoretically.[19] MXenes have been extensively researched due to their exciting prospects for pushing the innovative boundaries of technology development in the realm of low-dimensional materials, particularly in the field of electrochemical sensors. In contrast to other 2D materials, MXene has distinct electronic and metallic conductivity down to a single monolayer, which is critical for heterogeneous electron transfer between the modified electrode and the analyte, an essential feature for its use in electrochemical sensors.[20,21] The most intensively studied MXene, titanium carbide, showcases an exceptionally high metallic conductivity and surface area, which is highly desirable for low-noise and high-fidelity biosensors.[18,21] Apart from this, preliminary findings on the cytocompatibility and biocompatibility of MXenes (particularly for $Ti_3C_2T_x$) show no appreciable apoptosis, cytotoxicity, or hemolytic damage.[22,23] It is noteworthy that the surface termination groups enable the beneficial functionalisation of MXene, which attracts particular analytes in the presence of various interfering species in complex biological fluids.[24] Moreover, the enormous surface area of MXene is attributed to the interfacial contact between the electrode and electrolyte, enhancing the sensitivity of the electrode during sensing.[25,26] The substantial surface area of MXene has facilitated enhanced mass transfer and rapid charge kinetics, thereby surpassing the high overpotentials observed in conventional electrochemical transducers.[27]

Following the discovery of MXene, the first and foremost electrochemical sensor based on Ti_3C_2, an enzymatic biosensor for detecting H_2O_2, was developed in 2014.[28] The large specific surface area, superior biocompatibility, and hydrophilic surface are promising attributes of an immobilisation matrix in fabricating enzyme-based biosensors, as observed with Ti_3C_2 MXene. The organ-like structure of MXenes drives enzymes to the interior of the nanolayers, while surface terminations (such as hydroxyl groups) stimulate enzyme adsorption onto the surface, thereby increasing immobilisation. The peculiar MXene structure also fosters enzyme entrapment while increasing the likelihood of successful collisions between the substrate and redox protein; moreover, it minimises the chance of

enzyme detachment during substrate reaction.[21,29] However, the complexity of the immobilization of enzymes, the stability of the electrodes, and the high cost of fabrication hamper the development of MXene-based enzymatic electrochemical sensors. For this reason, the forefront research area focuses on the fabrication of non-enzymatic electrochemical sensors. To mention a few, F. Shahzad *et al.* created Ti_3C_2 MXene-modified GCE electrochemical sensors to achieve great sensitivity with a limit of detection (LOD) of 3 nM for detecting the neurotransmitter dopamine (DA) in real samples.[30] Recently, $Ti_3C_2T_x$ dip coated on an e-waste liquid crystal display was demonstrated to exhibit selective and sensitive detection of DA.[31] This approach proclaims the viability of MXene-mediated reuse of e-waste to fabricate sustainable electrochemical devices.

The inherent surface terminations arising from the etching process of MXene render exceptional hydrophilicity indispensable for stable dispersions in aqueous or hydrophilic media.[32,33] Drop-casting is the most common method for creating modified electrodes, which necessitates preparing a highly stable and well-dispersed coating solution.[34] The excellent solution dispersibility of MXene inks is highly useful in fabricating electrodes for electrochemical sensors by drop-casting techniques. Besides surface terminations, intercalants used for delamination have also been observed to influence the conductivity of MXenes significantly. Fig. 1 summarises some of the critical characteristics of MXenes that make them suitable for fabricating electrochemical sensors with high selectivity and nanomolar scale detection limits. Despite their noteworthy features, pure MXenes have several constraints, such as restacking and poor oxidative stability, that restrict their efficacy in electrochemical sensors. Numerous techniques have been employed to enhance the desirable electrocatalytic characteristics of MXenes, including surface and interlayer engineering, doping, and the development of MXene heterostructures.[35,36] In addition, many researchers have also used MXene in conjunction with other materials, notably various nanomaterials, to create composites that reinforce the electrochemical performance of sensors.[27] The unique layered structures of Ti_3C_2 MXene nanosheets have a large surface area, which could offer ample space for functional material intercalation/anchoring, potentially increasing the applicability of MXene nanosheets as promising support materials. Moreover, by means of surface functional groups, MXenes facilitate bonding with other functional materials through van der Waals forces of attraction, covalent bonds, hydrogen bonds, and charge transfer.[37,38] Owing to these factors, there has been a surge in research into MXene-based composites for versatile applications, particularly for electrochemical sensors.

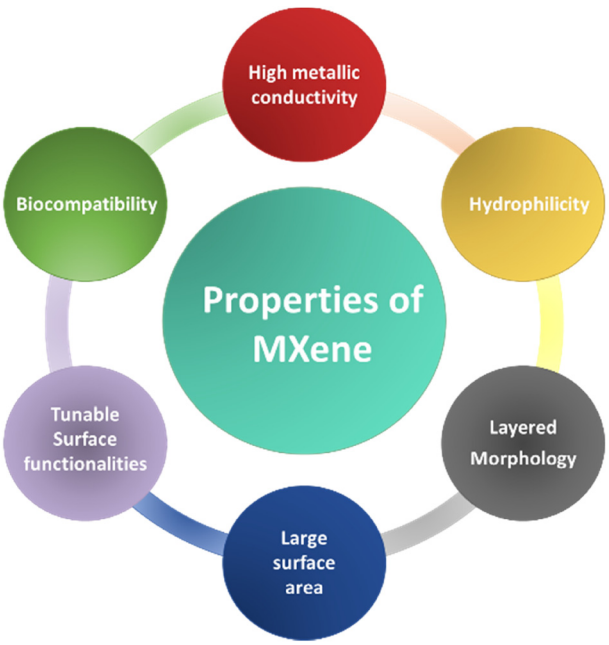

Fig. 1 Schematic illustration of the essential properties of MXenes concerning their use in electrochemical sensing.

3. MXene-nanocomposites as electrochemical sensors for clinically relevant biomarkers

3.1 General classification of MXene nanocomposites

MXenes have excellent prospects for various applications, ranging from sustainable energy technologies to point-of-care devices, because of their distinctive electronic/electrochemical, optical, mechanical, and chemical properties. Notably, the tunable electronic/electrochemical properties are achieved through careful intercalation or surface anchoring of functional materials onto MXenes. However, aggregation and self-restacking hamper the complete utilization of the tunable properties of MXenes for potential applications. Consequently, it is difficult to effectively inhibit the self-restacking of MXene while keeping its outstanding electrical conductivity to obtain MXene-related electrodes that are efficient for electroanalytical devices. Therefore, compositing MXenes with metal nanoparticles, metal oxides, conducting polymers, and carbonaceous materials is an innovative strategy to overcome the limitation of restacking while maintaining good conductivity.[39,40] On top of that, this could further enhance the oxidative stability of MXenes by preventing direct contact between MXene and oxygen from the surroundings. Furthermore, compositing MXenes with active nanostructures aids in tailoring the electrochemical activities, particularly toward detecting specific analytes, and thereby helps in developing electrochemical sensors with improved sensitivity, selectivity, and stability.[24] Fig. 2 presents the different categories of MXene-based nanocomposites with materials of superior electrochemical characteristics. The aforementioned MXene-based composites are synthesized using a variety of processes, including hydrothermal or solvothermal methods and self-assembly.

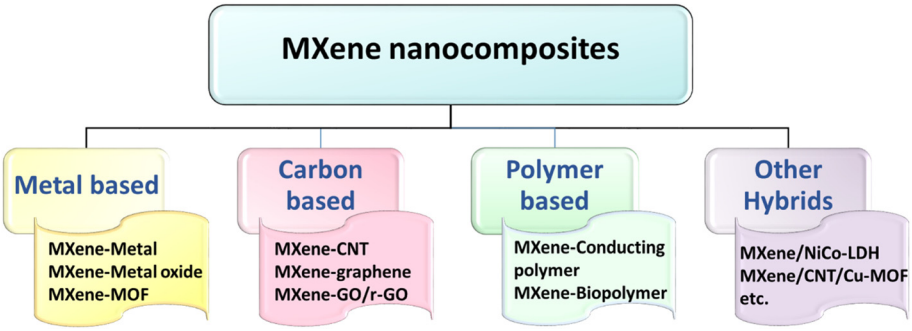

Fig. 2 The graphical presentation of different categories of MXene-nanocomposites reported as electrode materials for electrochemical sensing of clinically relevant biomarkers.

The superiority of MXene surface groups in reducing metal ions to metal nanoparticles is reported to be successful in decorating MXene surfaces with active transition metals/metal oxides. Furthermore, one of the major limitations, the instability of MXenes at higher anodic potentials, can be eliminated by incorporating electrochemically active transition metals. The spontaneous reduction of noble metal ions such as platinum (Pt) and palladium (Pd) on MXene exhibited attractive electrochemical sensing of biomolecules.[41,42] Similarly, silver (Ag) and gold (Au) nanoparticles with high conductivity and catalytic properties are being added to MXene to create hybrid MXene–metal nanostructures with several advantages such as more active surface sites, larger pore volume, and specific surface area.[43] The synergistic influence of transition metal doping on the interlayer separation of MXenes and electrochemical activity has been explored for the detection of biomolecules electrochemically. In addition, metal oxide nanoparticles such as TiO_2, Mn_3O_4, MnO_2, Co_3O_4, *etc.*, are intensively investigated as surface modifiers for MXene.[39,44] The synergic effect between MXene and these two materials improves the ionic conductivity and electron transfer rate capabilities of MXene materials for various electrochemical applications.[45,46] Recently, a one-pot electrostatic self-assembly of MOF-encased Ti_3C_2 improved the electronic conductivity of the composites due to the unidirectional charge mobility of Ti_3C_2.[47] $Ti_3C_2T_x$-templated *in situ* growth of a zeolite imidazole framework (cobalt-based MOF, ZIF-67) helped in intertwining the advantages of unique electrocatalytic activity and higher electronic conductivity resulting in excellent electrochemical response towards glucose oxidation.[48] Because of the electrostatic attraction of oxygenic groups of $Ti_3C_2T_x$, Co^{2+} ions were bound to the surface of MXene. The highly crystalline ZIF-67 was formed *in situ* on $Ti_3C_2T_x$ *via* the coordination interaction of Co^{2+} with the nitrogen atom of 2-methylimidazole, resulting in a $Ti_3C_2T_x$/ZIF-67 nanocomposite.[48]

Similarly, introducing other interlayer spacers, such as carbon nanotubes (CNTs), can preserve the hexagonal stacking of MXene sheets while providing more conductive paths for electron passage with reduced interfacial friction.[27] Besides, alternative forms of conductive and carbon-based materials, such as graphene, graphene oxide, and reduced graphene oxides (rGO), are frequently integrated into various MXenes to improve physical, structural, and electrochemical characteristics subjected to the intended application.[40,49] For instance, a one-step hydrothermal approach was utilised to successfully generate an MXene/N-rGO composite, which was then used to modify a glassy carbon electrode (GCE) for electrochemical detection of adrenaline.[50] Primarily, mild sonication was used to disperse MXene in deionized water, followed by ethylenediamine reduction of graphene oxide. The resultant aqueous dispersion was then transferred to a Teflon-lined autoclave for 24 hours of sustained heating at 180 °C to obtain MXene/N-rGO composites. Polymers endow MXene with specific functions, providing abundant electron–ion channels and interaction sites and thereby improving the performances of the composites.[51] Therefore, conducting polymers such as polyaniline, polypyrrole (PPy), polyacetylene, poly(3,4-ethylenedioxythiophene) (PEDOT), and polyphenylene can be composited with MXenes by several methods like solvent blending, casting, filtration, *in situ* polymerization, and melt blending. Moreover, assembling hybrid materials allows for combining beneficial properties unavailable in traditional forms.[52] The intricate chemical interactions between the functional molecules and MXene surfaces promote the formation of hybrid structures through self-assembly.[53] An electrostatic interaction between positively charged poly(diallyldimethylammonium chloride) (PDDA) and negatively charged $Ti_3C_2T_x$ resulted in the self-assembly of $Ti_3C_2T_x$/PDDA composites with excellent energy storage.[54] A simple hydrothermal approach was also employed to fabricate MXene/NiCo-LDH nanocomposites for a non-enzymatic glucose sensor. The precursors were dispersed in a solvent mixture containing methanol and ultrapure water, and the mixture was magnetically stirred at room temperature before being hydrothermally reacted in a Teflon-lined autoclave at 180 °C for 24 hours to obtain the nanocomposite.[55] Although hydrothermal treatment has shown to be a simple synthesis process, the aqueous environment may result in O_2 and H_2O-induced reactions that result in the oxidation

of Ti_3C_2 MXene. As a result, this technique is a poor choice for producing extremely specific MXene-based composites.[56] Meanwhile, the solvothermal approach eliminates the oxidation features seen in hydrothermal treatment. This demonstrates the successful synthesis of materials with diverse morphologies, making it an ideal synthesis route for constructing MXene-based composites.[53] Detailed discussions on the application of MXene nanocomposites for various electrochemical sensing of potential biomarkers have been presented in the forthcoming sessions.

3.2 MXene–metal nanocomposites as electrochemical sensors

The multilayer structure of MXene allows it to support precious metal nanoparticles and avoid the aggregation of nanoparticles.[57] Based on this, Chen *et al.* developed an electrochemical biosensor by loading L-cysteine-terminated

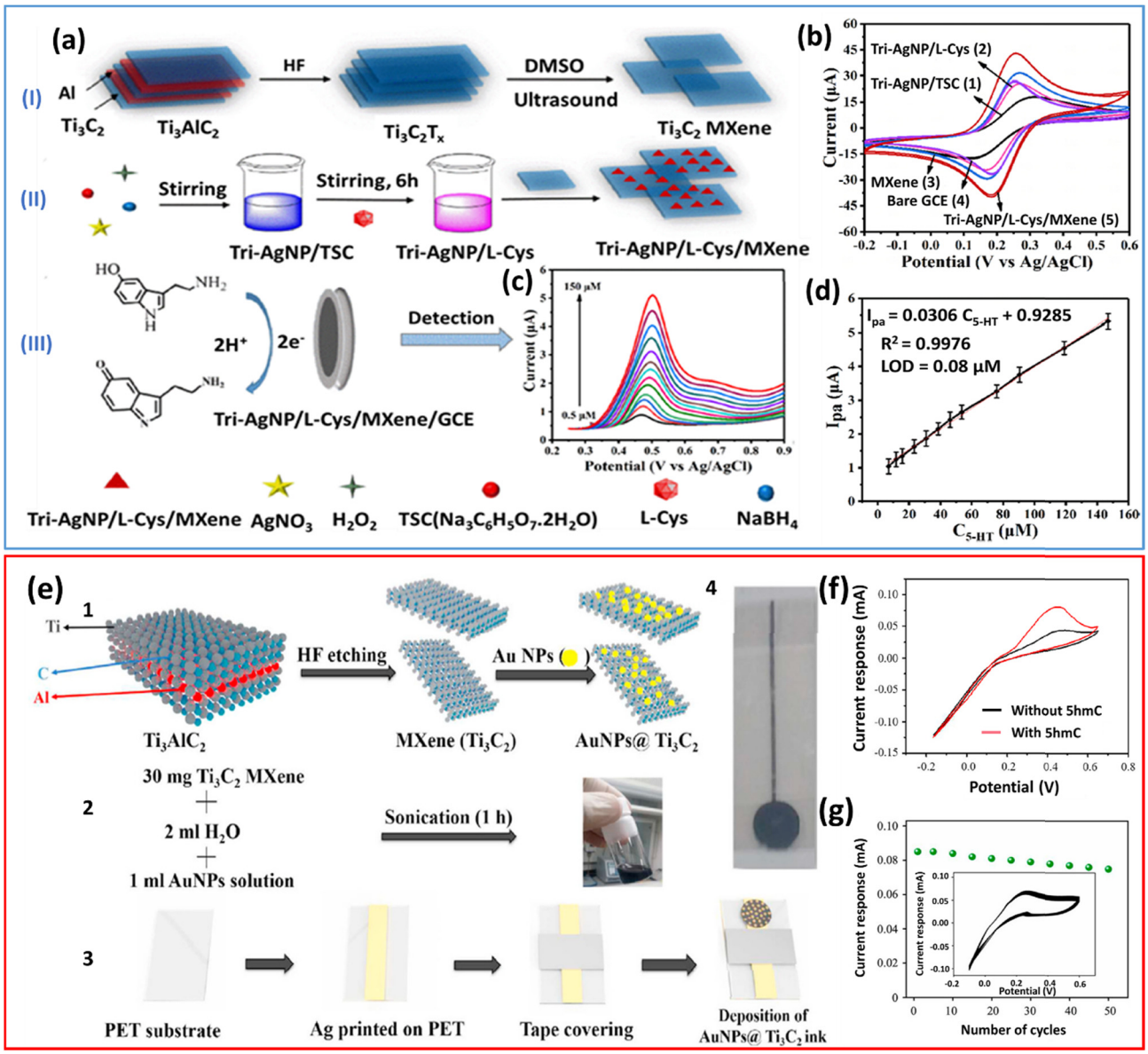

Fig. 3 a) Mechanism of preparation of Tri-AgNP/L-Cys/$Ti_3C_2T_x$ nanocomposites for detecting 5-HT.(I) Preparation of multilayer Ti_3C_2 MXene, (II) preparation of Tri-AgNP/L-Cys/MXene, and (III) detection of 5-HT by Tri-AgNP/L-Cys/MXene. b) CV curves for Tri-AgNP/TSC/GCE, Tri-AgNP/L-Cys/GCE, MXene, bare GCE, and Tri-AgNP/L-Cys/MXene/GCE; tests carried out in 0.1 M KCl solutions containing 1.0 mM $Fe[(CN)_6]^{3-}/^{4-}$. c) DPV of 5-HT with changing concentration as 0.5, 7.0, 12, 16, 23, 31, 39, 46, 54, 76, 90, 119, and 150 μM. d) Relationship between peak current (I_{pa}) and concentration of 5-HT. (a to d) Reproduced with permission from ref. 58. Copyright (2021) American Chemical Society. e) (1 and 2) Schematic diagram of the preparation of AuNPs@Ti_3C_2 MXene ink, 3) fabrication of the sensor device, and 4) printed AuNPs@Ti_3C_2 MXene sensor device. f) Current response of AuNPs@Ti_3C_2 MXene to genomic DNAs without 5hmC (black curve) or with 5hmC (red curve). g) Plot of current response of AuNPs@Ti_3C_2 MXene sensor incubated with 5hmC-containing DNAs against number of cycles; inset: cyclic voltammogram depicting the sensor stability after multiple runs (up to 50 cycles). (e to g) Reproduced with permission from ref. 59. Copyright (2022) Elsevier.

triangular silver nanoplate (Tri-AgNP/L-Cys) on the surface and between the layers of $Ti_3C_2T_x$ MXene to detect 5-hydroxytryptamine (5-HT)[58] (Fig. 3a). The loading of Tri-AgNP helps to overcome the restacking issue of layered $Ti_3C_2T_x$, thereby increasing the specific surface area, facilitating electron transport, and improving the electrochemical performance. To fabricate Tri-AgNP/L-Cys, trisodium citrate (TSC) terminated AgNPs were prepared initially, followed by selective replacement of TSC with thiol L-Cys (Fig. 3aI and II). Eventually, adding MXenes with high conductivity, surface area, and chemical stability improves the electrical response of Tri-AgNP/L-Cys/MXene to 5-HT (Fig. 3b). The synergy of Tri-AgNP/TSC, L-Cys, and MXene provides additional active sites for the electrocatalytic oxidation process of 5-HT. The differential pulse voltammetry (DPV) employed for detecting 5-HT in a linear concentration regime of 0.5–150 μM provided an LOD of 0.08 μM (Fig. 3c and d). The sensor was also influential in detecting 5-HT in the human blood serum samples, and the recovery rate was 95.38–102.3%.

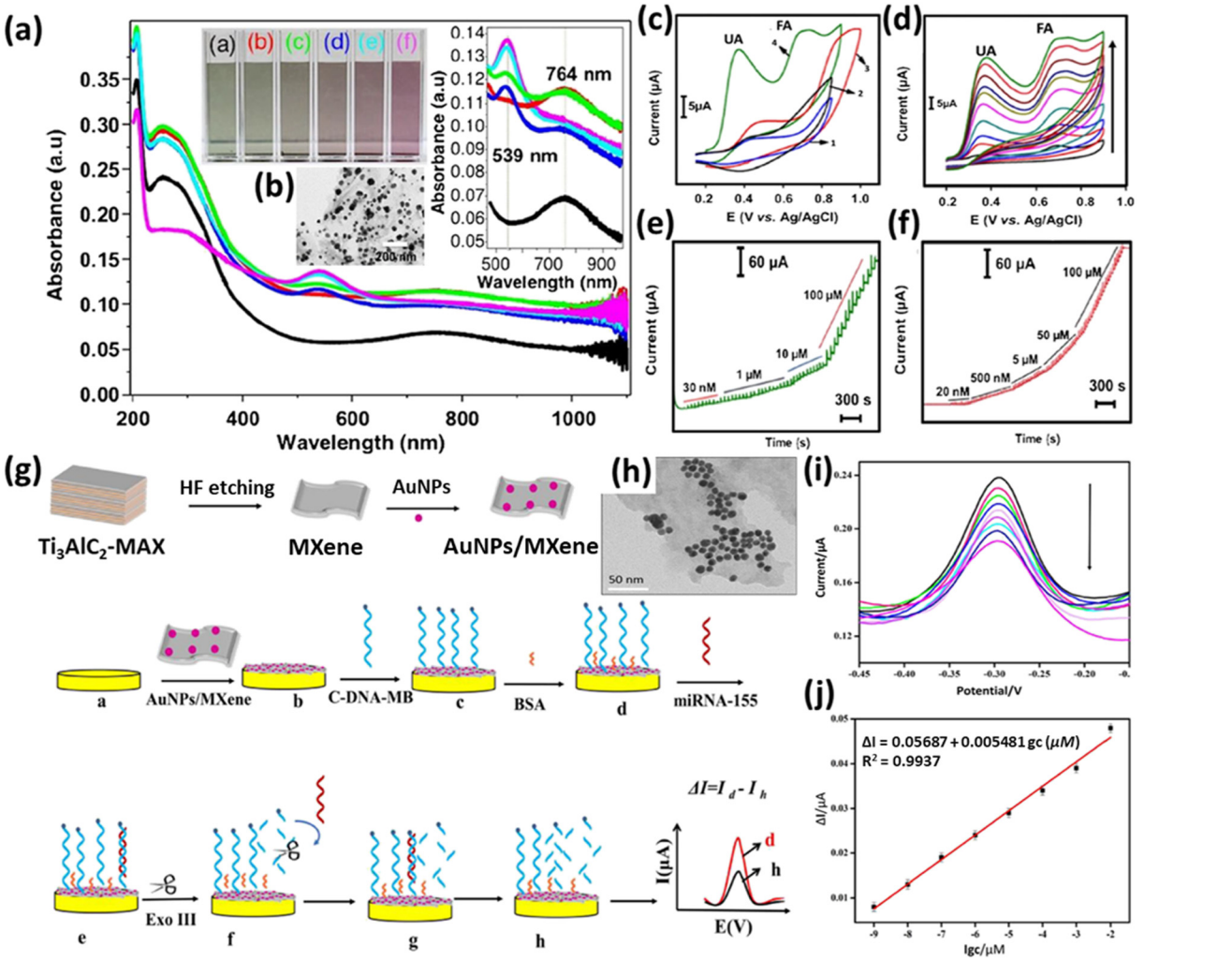

Fig. 4 (a) UV-visible-NIR spectroscopy analysis on delaminated $Ti_3C_2T_x$ flakes and spontaneous reduction of gold nanoparticles (AuNPs) onto delaminated $Ti_3C_2T_x$ (AuNP@$Ti_3C_2T_x$); inset: magnified UV spectra from 500 nm to 900 nm. The enclosed photographic images (a to f) show the colloidal suspension of AuNP@$Ti_3C_2T_x$ hybrids synthesized by adding different concentrations of gold ion solution in the colloidal delaminated $Ti_3C_2T_x$-MXene solution for the production of AuNPs on $Ti_3C_2T_x$ flakes. (b) HR-TEM images of the AuNP@$Ti_3C_2T_x$ hybrid produced by adding 70 μM of gold ion solution; scale bar is 200 nm. (c) CVs of (1) unmodified GCE, (2) AuNP, (3) $Ti_3C_2T_x$ and (4) AuNP@$Ti_3C_2T_x$ hybrid at the GCE toward 3 μM UA + 3 μM FA dissolved in 0.1 M phosphate buffer (pH 7.0). (d) The increasing concentrations of both UA and FA added and the corresponding CVs recorded using the modified GCE electrode in 0.1 M phosphate buffer, with a scan rate of 50 mV s^{-1}. (e) Amperometric *i*–*t* curves of the modified GCE electrode upon each addition of UA into phosphate buffer (pH 7.0) and (f) amperometric response of the modified GCE electrode for FA. (a to f) Reproduced with permission from ref. 60. Copyright (2019) Springer Nature. (g) Schematic representation of the electrochemical miRNA-155 biosensor based on the AuNPs/Ti_3C_2 MXene 3D nanocomposite developed by the Exo III-aided cascade target recycling methodology a) AuE b) AuNPs/Ti_3C_2 MXene/AuE c) C-DNA/AuNPs/Ti_3C_2 MXene/AuE d) BSA/C-DNA/AuNPs/Ti_3C_2 MXene/AuE e) miRNA-155/BSA/C-DNA/AuNPs/Ti_3C_2 MXene/AuE f–h) Exo III/miRNA-155/BSA/C-DNA/AuNPs/Ti_3C_2 MXene/AuE. (h) TEM image of AuNPs/Ti_3C_2 MXene nanocomposite; scale bar is 50 nm (i) DPV curves in response to different miRNA concentrations from 0.0 to 10 nM (tests were carried out in 0.2 M PBS buffer at a solution pH of 7.4). (j) The linear relationship between the current variation Δ*I* and the negative logarithm of the miRNA-155 concentration. (g to j) Reproduced with permission from ref. 61. Copyright (2020) Elsevier.

Likewise, among the noble metal catalysts, AuNPs are widely used for sensing biological molecules due to their excellent conductivity, biocompatibility, and simple surface functionalization possibilities. A novel printable electrochemical sensor based on AuNPs@Ti_3C_2 nanocomposites has been reported for discriminating 5-methylcytosine (5mC) and 5-hydroxymethylcytosine (5hmC) enriched deoxyribonucleic acid (DNA).[59] The sensor was fabricated by printing a highly conductive and adhesive silver ink using nozzle-jet printing onto a polyethylene terephthalate (PET) substrate, followed by dropcasting of AuNPs@Ti_3C_2 ink at one end (Fig. 3e). In addition to differentiating 5hmC and 5mC, the sensor could also consistently and rapidly monitor the 5hmC decrease in the genome of tumour cells (Fig. 3f and g).

S. Elumalai *et al.* reported the solution-processing-based galvanic deposition of AuNPs on delaminated $Ti_3C_2T_x$ sheets to obtain a colloidal suspension of AuNP@$Ti_3C_2T_x$.[60] This synthesis strategy followed the spontaneous reduction of gold nanoparticles onto delaminated $Ti_3C_2T_x$ nanosheets (AuNP@$Ti_3C_2T_x$) devoid of reduction agents or surfactants. The spontaneous reduction of Au^{3+} ions to Au NPs onto the delaminated $Ti_3C_2T_x$ flakes was confirmed by ultraviolet-visible-near infrared (UV-vis-NIR) spectroscopy and high-resolution-transmission electron microscopy images (HR-TEM) (Fig. 4a and b). As a result of Au NP adsorption, the AuNP@$Ti_3C_2T_x$ composite serves as a template for the strong electrocatalytic activity of the analyte (Fig. 4c). The modified GCE electrode demonstrated considerably improved electrocatalytic peak currents at a reduced oxidation potential, indicating that the customized interface had an exceptional electrocatalytic performance against uric acid (UA) and folic acid (FA) with lowered detection limits to nM concentrations (Fig. 4d–f). A novel electrochemical biosensor based on AuNPs/Ti_3C_2 MXene nanocomposite for sensitive miRNA-155 detection by exonuclease III (Exo III)-aided cascade target recycling has been reported (Fig. 4g).[61] The distribution of loaded AuNPs onto Ti_3C_2 MXene nanosheets is shown in Fig. 4h. MicroRNAs (miRNAs) are critical indicators for the early detection and prognosis of genetic disorders such as tumours in humans and neurological diseases. Among the miRNAs, miRNA-155, widely recognised as involved in lymphoma, is also now implicated in advancing breast cancer, and the strategy developed here is employed as a versatile tool for miRNA detection in bioanalysis (Fig. 4i). The AuNPs/Ti_3C_2 MXene 3D nanocomposite has a high surface area for capture DNA (C-DNA) loading and allows for electron transport between the electrochemical species, methylene blue, and the underlying electrode surface. Under some conditions, one miRNA-155 chain releases multiple C-DNAs with the help of Exo III-aided cascade target recycling amplification, resulting in high sensitivity with a detection limit as low as 0.35 fM (Fig. 4j). Pristine $Ti_3C_2T_x$ fails to show adequate stability in the anodic potential window. An irreversible anodic peak appears at an applied voltage of roughly +430 mV *vs.* Ag/AgCl, suggesting irreversible oxidation of $Ti_3C_2T_x$, which could not be re-reduced.[62] Surface modification is an efficient method for stabilising MXenes in the anodic potential window. A GCE modified with Pd@$Ti_3C_2T_x$ has been reported by Rasheed *et al.* as a stable and extremely sensitive electrochemical sensor for the detection of L-Cys, which is a potential biomarker for the diagnosis of cancer, Parkinson's and Alzheimer's illnesses, and acquired immune deficiency syndrome.[41] The sensor was used to detect L-Cys in an aqueous medium and was made by casting a Nafion-stabilized layer of the Pd@$Ti_3C_2T_x$ nanocomposite onto a GCE. Pd NPs are used to increase the stability of $Ti_3C_2T_x$ and the electrocatalytic activity for L-Cys detection. The sensor also showed high selectivity against typical interfering ions such as uric acid, dopamine, ascorbic acid, and glucose.

The presence of numerous functional groups on MXenes, along with its role as a conductive matrix and reducing agent, eliminates lattice mismatching and facilitates the straightforward synthesis of various metal-modified nanostructures.[58] Furthermore, the high surface area MXene nanosheets function as a two-dimensional substrate, and the many terminal groups chemically attach the metals with great stability to create encapsulated, loaded, or sandwiched nanostructures with improved properties and stability. Generally, metal nanoparticles are absorbed onto the surface of MXene through electrostatic interaction to generate decorated MXene hybrid structures.[41] Optimal metal doping of MXene effectively enhances the electrochemical performance by increasing the interlayer distance, providing more electrochemically active sites and thus rendering them particularly appealing for electrochemical detection of specific analytes with improved selectivity and current response.

3.3 MXene–metal oxide and MXene–MOF nanocomposites as electrochemical sensors

Metal oxides and MOFs have been recently used as electrochemical sensing platforms to detect specific analytes because of their distinctive characteristics, such as high porosity and abundant metal active sites. The high levels of reactive oxygen species (ROS), H_2O_2, can serve as a cancer biomarker in the body fluids. A simple and accurate electrochemical sensor using MXene–Co_3O_4 and a screen-printed electrode (SPE) was developed by S. Singh *et al.* to measure changes in H_2O_2 in cancer cells.[63] As shown in Fig. 5a, the MXene–Co_3O_4-modified SPE has been used to measure ROS levels in cancerous cell lines corresponding to breast and prostate cancers. The cyclic and linear sweep voltammetry (CV and LSV) was employed to quantify the H_2O_2 present, and the LOD was found to be 0.5 μM (Fig. 5b and c). MXene allows for enhanced electron conductivity, and the presence of Co_3O_4 provides a catalase-like activity toward H_2O_2, thus optimising sensitivity and selectivity, respectively (Fig. 5d). An innovative portable electrochemical device was created and has demonstrated the ability to assess H_2O_2 fluctuation in cancer cells modified with transforming growth factor in

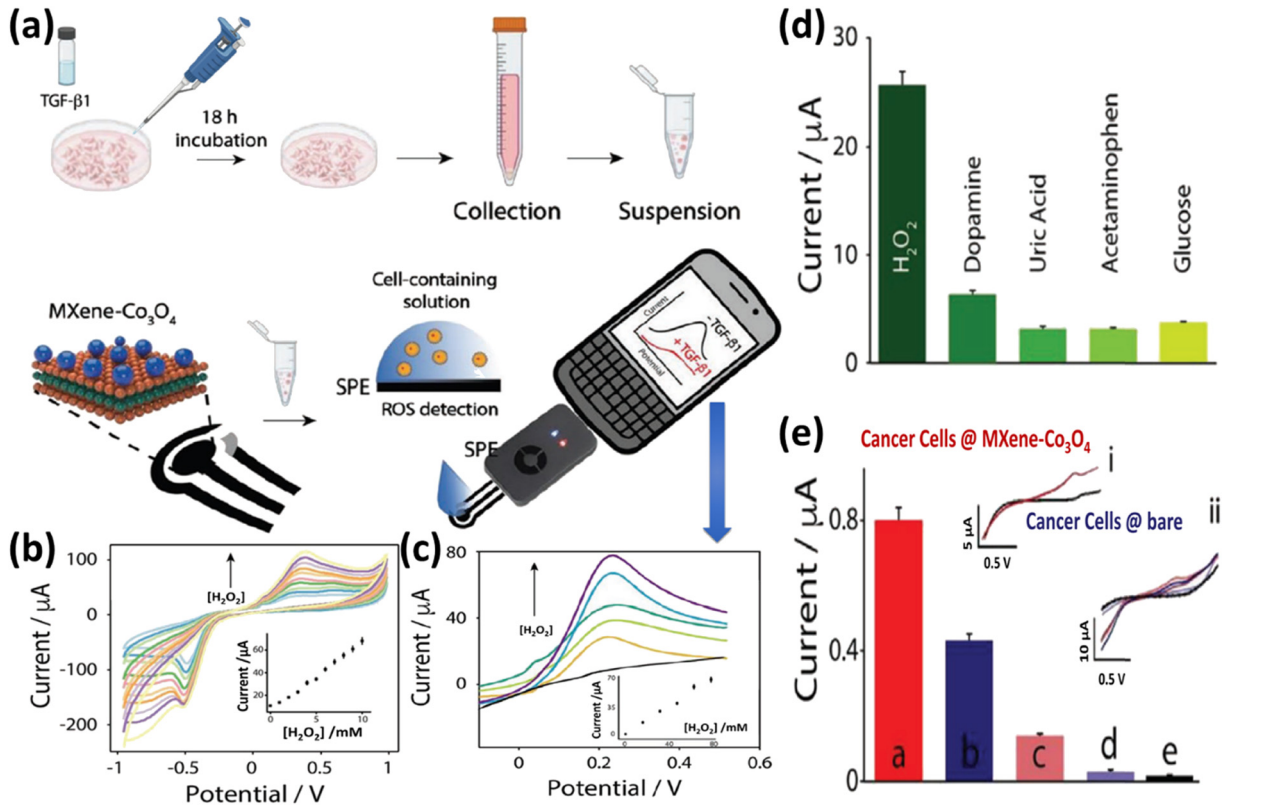

Fig. 5 a) Illustration of monitoring ROS in cancer cells using the MXene–Co_3O_4-nanocomposite designed and integrated onto a screen-printed electrode. b) Cyclic voltammetry studies of the MXene–Co_3O_4 modified SPE using various concentrations of H_2O_2 up to 10 mM at a scan rate of 50 mV s^{-1}; inset: calibration curve of peak current value plotted against H_2O_2 concentrations up to 10 mM. c) LSV of electrochemically activated MXene–Co_3O_4 modified SPE in 0.1 M KCl with various H_2O_2 concentrations (up to 75 μM); inset: calibration curve of peak current value plotted against H_2O_2 concentrations. d) Specificity testing in 0.1 M KCl with 10 μm H_2O_2 and interferents dopamine, uric acid, acetaminophen, and glucose. e) Electrochemical detection of ROS produced by a) DU145 cell lines, b) MDA-MB-231 cell lines, and in c) DU145 cell lines treated with TGF-β1, d) MDA-MB-231 cell lines + TGF-β1, and e) human immortalized keratinocyte cell line HaCat. Inset i: Measurements with the nanocomposite in the presence of cancer cells (red) and with a non-modified electrochemical platform (black). Inset ii: Voltammetric measurements relative to histograms. Reproduced with permission from ref. 63. Copyright (2023) Wiley-VCH.

real-time. MXene–Co_3O_4-modified SPEs are more sensitive to prostate cancer cell lines (Fig. 5e) than breast cancer cell lines, indicating that the nanocomposite developed present in the decentralized device can distinguish between cancer cells. Tin dioxide quantum dots (SnO_2 QDs), an ultrasmall semiconductor nanomaterial, have several benefits over other metal oxides, including easy synthesis, no toxicity, and superior electrical conductivity. Furthermore, due to the quantum size effect, ultrasmall SnO_2 QDs as an electrode modifier could provide additional active sites and improve the reaction rate.[64] In light of this, Shi *et al.* synthesised SnO_2 QDs@Ti_3C_2 nanocomposites using a facile *in situ* growth method.[65] The obtained composite was used to modify the GCE to detect DA. SnO_2 quantum dots for the composite preparation were produced through the hydrolysis of $SnCl_2$. The interlayer surface of Ti_3C_2 MXene was uniformly covered with SnO_2 QDs, which increased the electroactive surface area and the electron transfer capacity. Compared to earlier studies on electrochemical sensing of DA, the SnO_2 QDs@Ti_3C_2 MXene/GCE sensor exhibited a very low detection limit. Moreover, the sensor successfully detected DA in human urine and serum samples.

MOFs are recognized as efficient, affordable, and environment friendly solutions for various electrochemical applications, much like metal oxides. Despite the high electrochemical activity of MOFs, their poor electrical conductivity would significantly reduce their sensitivity, which can be overcome by compositing with MXene. Therefore, Xuhui Han *et al.* reported a Co-based MOF (ZIF-67) on 2D MXene ($Ti_3C_2T_x$/ZIF-67 nanocomposite) with excellent conductivity for the electrochemical analysis of glucose.[48] The $Ti_3C_2T_x$/ZIF-67 nanocomposite was synthesised by loading the porous Co-based MOF (ZIF-67) on 2D MXene using a facile *in situ* method (Fig. 6a). Fig. 6b illustrates the homogeneous distribution of ZIF-67 nanoparticles on the surface of $Ti_3C_2T_x$ nanosheets. The process started with the oxidation of Co(II) to Co(III), which was followed by the oxidation of glucose molecules to gluconolactone through Co(III), and finally, the reduction of Co(III) to Co(II) (Fig. 6c). This research demonstrated a practical approach for creating

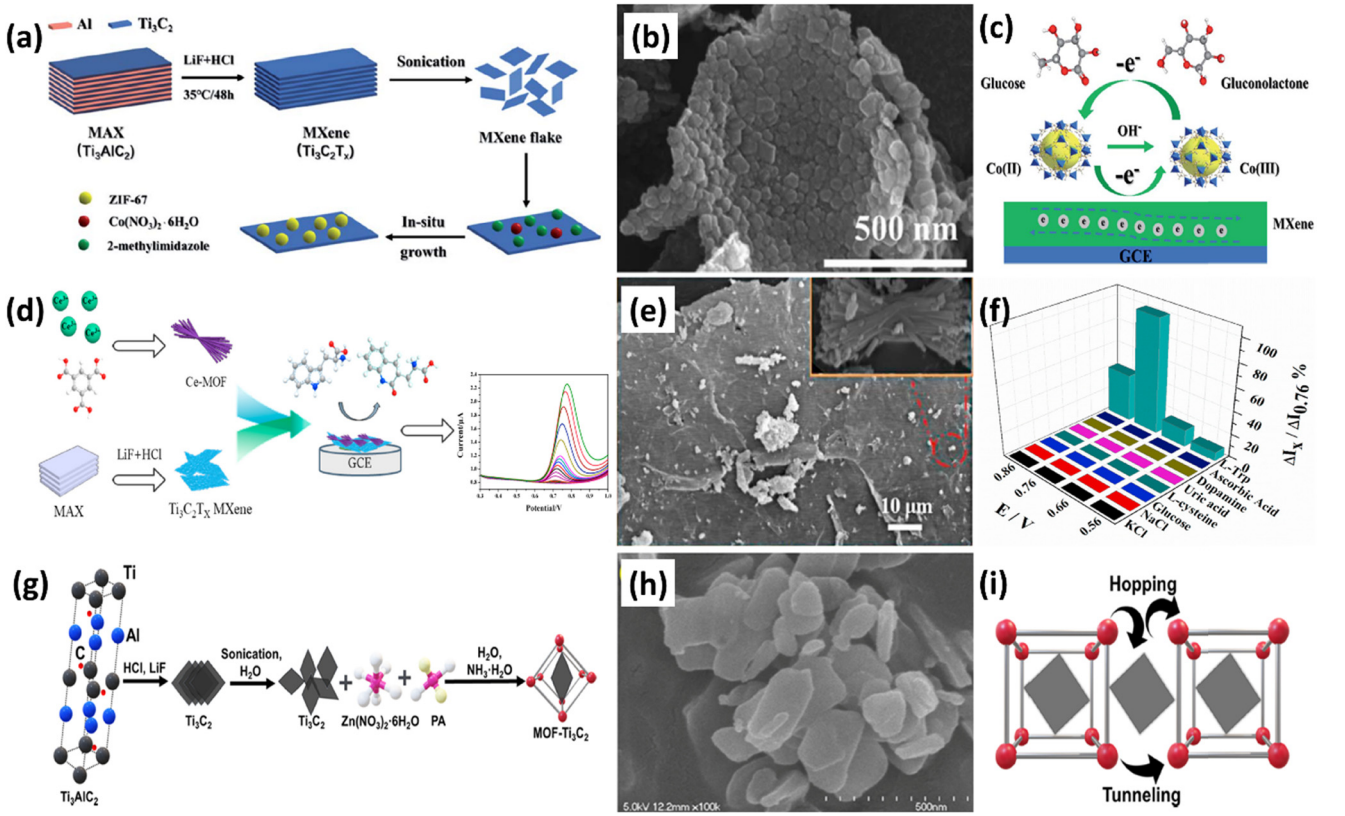

Fig. 6 a) The synthetic process of the $Ti_3C_2T_x$/ZIF-67 nanocomposites. b) SEM image of the $Ti_3C_2T_x$/ZIF-67 nanocomposite. c) The mechanism of $Ti_3C_2T_x$/ZIF-67/GCE to detect glucose in NaOH solution. (a to c) Reproduced with permission from ref. 48. Copyright (2022) Royal Society of Chemistry. d) Preparation of the Ce-MOF/$Ti_3C_2T_x$ MXene composite and modified electrode. e) SEM image of the Ce-MOF/$Ti_3C_2T_x$ MXene composite; inset: the magnified image of the encircled area. f) Ce-MOF/$Ti_3C_2T_x$ MXene/GCE 1 : 2 selectivity profile with L-Trp (50 μM), ascorbic acid (50 μM), dopamine (50 μM), uric acid (50 μM), L-cysteine (50 μM), glucose (100 μM), KCl (100 μM), and NaCl (100 μM). (d to f) Reproduced with permission from ref. 66. Copyright (2022) Elsevier. g) Schematic of the synthesis of the MOF–Ti_3C_2 composite *via* an electrostatic self-assembling technique in distilled water at room temperature. h) SEM image of MOF–Ti_3C_2. i) Hopping and tunnelling charge transfer mechanism in solid state-ordered porous materials (SSOPMs), including metal–organic frameworks (MOFs). (g to i) Reproduced with permission from ref. 47. Copyright (2023) Elsevier.

high-performance electrochemical sensors, combining good electrocatalytic active MOFs with high conductivity 2D $Ti_3C_2T_x$. Chen *et al.* fabricated a Ce-MOF/$Ti_3C_2T_x$ composite as an electrode active material for the electrochemical detection of L-tryptophan (L-Trp).[66] A three-dimensional straw-sheaf-like Ce-MOF was joined with a few layered $Ti_3C_2T_x$ nanosheets, as shown in Fig. 6d. The presence of metal active sites and a high surface area of Ce-MOF achieve outstanding electrocatalytic oxidation of L-Trp. The straw-sheaf-like structure can provide good capacity for L-Trp adsorption (Fig. 6e). The modified electrode demonstrated a strong current response even in the co-existence of L-Trp with interferents (ascorbic acid, dopamine, uric acid, L-cysteine, glucose, KCl, and NaCl) (Fig. 6f), which indicates that the common interfering substances did not affect the measurement of L-Trp. Paul and his colleagues used a non-conductive MOF ($[Zn_4(btec)_2(H_2O)_6]_n \cdot 3nH_2O$) and Ti_3C_2 for the detection of dopamine (DA),[47] which is a crucial biomarker for several neurological diseases. The one-pot electrostatic self-assembling method was used to create the MOF–Ti_3C_2 composite in distilled water (Fig. 6g). Due to the unidirectional charge mobility, the MOF physically bonded around the Ti_3C_2 sheet improves electrical conductivity. The nanocomposite produced has a high crystallinity with a structure of conjugated orbitals of charge donors and acceptors, which improves electron flow. The major factor driving electrochemical sensing here is space charge transfer (Fig. 6h and i); hence the important goal is to create a highly conjugated, charge-carrying, crystalline, and defect-free MOF–Ti_3C_2 composite for DA sensing. This technique was utilised to identify DA in PBS that contained ascorbic acid (AA) and 5-amino valeric acid (VA). With a LOD of 110 nM, the material developed identified DA at concentrations between 90 and 130 nM. Based on the above mentioned studies, MXene demonstrates itself to be an optimal material for appropriate hybridization with metal oxides or MOFs. MXene as a conductive substrate facilitates the self-assembly or *in situ* formation of metal oxide nanostructures, hence improving the electrocatalytic properties and conductivity. Combining MXenes with MOFs in an optimised manner not only addresses the limitations of MOFs (such as low electrical conductivity and poor stability), but also introduces new functionalities

by combining MOF's extensive surface area, adjustable porous structure, numerous exposed REDOX active sites, non-toxicity, and MXene's high electrical conductivity and environmental protection.

3.4 MXene–carbon based composites as electrochemical sensors

Carbon-based materials such as graphene, rGO and CNTs can be used to improve the electrochemical performance of MXene due to their high electronic conductivity, flexibility, and proton exchange.[67] Furthermore, the carbon-based materials introduced into $Ti_3C_2T_x$ can function as spacers, reducing nanosheet restacking and increasing the interlayer spacing between $Ti_3C_2T_x$ layers, which helps to stabilise the layer structure. A GCE modified with the $Ti_3C_2T_x$–rGO nanocomposite was developed by hydrazine reduction followed by a self-assembly process, and its electrochemical sensitivity to various serotonin concentrations was investigated using the differential pulse voltammetry (DPV) method.[68] The single-layer open structure of the $Ti_3C_2T_x$–rGO nanocomposite provides an extensive surface area and abundant active sites for serotonin adsorption, which is advantageous for its electrochemical oxidation. The developed sensor successfully assessed serotonin levels in human plasma samples, suggesting that this detection method is likely to be employed to prevent and promptly diagnose serotonin-related diseases. J. Rajendran *et al.* used MXene/graphene film to detect nicotine electrochemically.[69] The electrochemical exfoliation of graphite into graphene

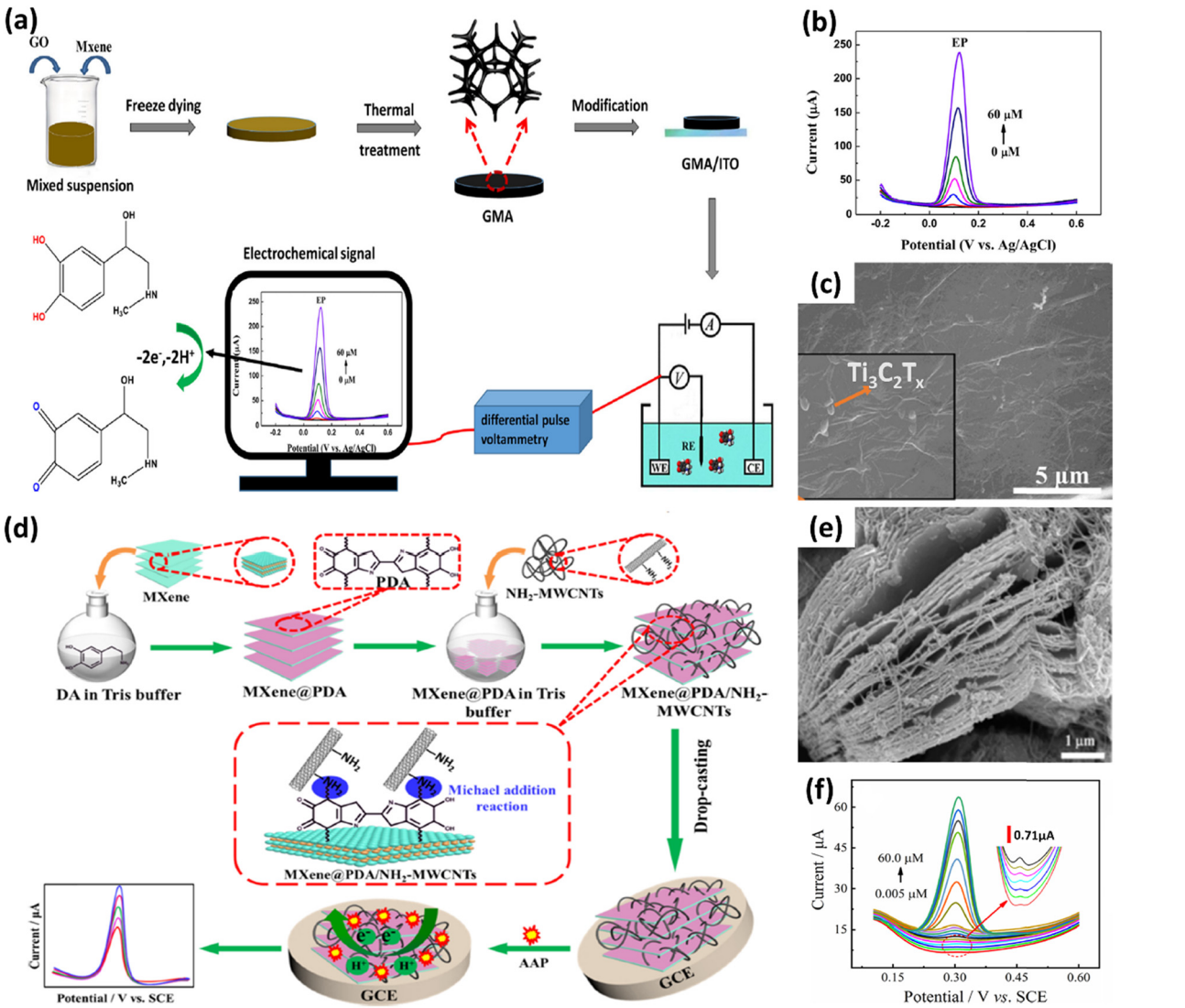

Fig. 7 a) Schematic of the GMA/ITO electrode preparation and electrochemical detection of epinephrine (EP). b) The DPV curves of the GMA/ITO electrode with various concentrations of EP. c) SEM image of the GMA. Inset: uniform distribution of $Ti_3C_2T_x$ nanoparticles on the surface of 3D graphene framework. (a to c) Reproduced with permission from ref. 71. Copyright (2021) Elsevier. d) Pictorial representation of the synthesis process of MXene@PDA/NH_2-MWCNTs/GCE for AAP determination. e) SEM image of MXene@PDA/NH_2-MWCNTs. f) DPV analysis with various AAP concentrations at MXene@PDA/NH_2-MWCNTs/GCE in 0.1 M PBS (pH 7.0). (d to f) Reproduced with permission from ref. 72. Copyright (2021) Elsevier.

and selective etching of Al from MAX resulted in the generation of graphene and MXene layers, respectively. The mild ultrasonication of these two components afterwards resulted in MXene/graphene dispersions. The functional groups such as carboxylic, epoxy, and hydroxyl of graphene surfaces substantially improved the stability of MXene dispersions.[69] Using DPV and amperometry, two linear ranges of 1 to 55 μM and 30–600 nM were observed for nicotine with the lowest LODs of 290 nM and 0.28 nM, respectively. Additionally, graphene can be doped with heteroatoms like nitrogen to enhance its electrical conductivity and electrochemical activity. Chen *et al.* employed a one-step hydrothermal method to synthesise the MXene/N-rGO composite, which was then used as the electrode material for adrenaline (AD) electrochemical sensing.[50] The doped nitrogen in rGO, bridges MXene and rGO through strong hydrogen bonds, which in turn enhances the electrocatalytic activity of the composite for oxidising AD. The sensor detected AD linearly from 0.01 to 90.0 μM with a LOD of 3.0 nM. The application of this sensor for voltammetric detection of AD in urine samples was also successful.

Unlike 2D graphene nanosheets, 3D porous graphene successfully prevents aggregation and exhibits superior qualities such as increased porosity, improved mechanical stability, and catalytic activity providing an effective framework for detecting small biomolecules.[70] A 3D porous rGO/$Ti_3C_2T_x$ MXene (GMA) was achieved using freeze-drying and heat treatment techniques[71] (Fig. 7a). The electrode was then used for the electrochemical detection of epinephrine (EP) (Fig. 7b). The 3D porous structure of GMA makes the entry of small biomolecules easier and increases the electrode–analyte interface (Fig. 7c). The electrode could also detect EP in human urine samples, indicating the employability of the electrodes for POC diagnostics. Similarly, another carbon-based compound, MWCNT, was composited with MXene to fabricate effective electrode materials for various electrochemical devices. The easy functionalisation, exceptional electrocatalytic performance, and strong electron transfer ability of MWCNT identify it as a valuable one-dimensional material for use as an intercalant in the interlayer of MXene. Thus far, MXene/MWCNT nanohybrids have been developed as efficient electrode materials for a range of electrochemical device applications. However, the interface binding of MXene and MWCNTs mostly depends on non-covalent electrostatic attraction and van der Waals forces, which would restrict the mechanical stability and reduce the electrochemical performance. A simple method for *in situ* cross-linking of amino functionalised multi-walled-carbon nanotubes on polydopamine functionalised MXene (MXene@PDA/NH_2-MWCNTs) was created (Fig. 7d) by Chen *et al.* to address this problem.[72] The NH_2-MWCNTs can be evenly and firmly distributed on MXene@PDA using the Michael addition reaction. To prevent the MXene stacking phenomenon, NH_2-MWCNTs are tightly linked to MXene@PDA and act as an interlayer barrier. The composite was used as an electrochemical sensing platform for detecting acetaminophen (AAP) because of its distinctive structure, abundant active sites, hierarchical mass transfer pathways, and outstanding electrocatalytic capabilities (Fig. 7e and f). As a result, the sensor exhibits wide linear ranges of 0.005 to 60.0 μM, as well as a low LOD of 1.0 nM. Furthermore, the fabricated sensor was effectively used to identify AAP in a urine sample and paracetamol tablet. In addition to demonstrating its potential as an alternative to conventional sensing materials with exceptional applicability towards the selective detection of versatile analytes, the aforementioned studies on developing MXene nanocomposites open up the feasibility of 2D MXenes to incorporate 1D, 2D, and 3D nanostructures to yield hybrid nanostructures.

3.5 MXene–polymer nanocomposites as electrochemical sensors

The formulation of MXene–polymer composites allows for the fine-tuning of the physical and chemical properties of MXene due to the abundance of surface functional groups compatible with the polymeric chains. Incorporating polymers can facilitate the assembly of MXene and functional polymers promoting interlayer space expansion, reducing the distance of ion/electron transport, and improving surface hydrophilicity.[73,74] Single-layer MXenes are more polymer-friendly and have more easily accessible surface hydrophilicity than their multilayered equivalents,[75] and thereby, MXenes are typically delaminated first before being combined with polymers. Based on this, Q. You *et al.* reported $Ti_3C_2T_x$/polypyrrole (MXene/PPy) nanocomposites for the simultaneous recognition of DA and UA under the interference of AA.[76] Aqueous acid etching was used to generate the multilayer $Ti_3C_2T_x$ MXene, which was then delaminated into a single-layer nanosheet to assist in the *in situ* development of PPy nanowires. The as-prepared sensor can quantitatively determine DA and UA because the diffusion mechanism regulates the catalytic oxidation of DA and UA. In aspiration of combining the features of MXene with PEDOT, Wustoni *et al.* electrochemically synthesised a PEDOT composite by incorporating MXene as a co-dopant along with poly(styrene sulfonate) (PSS).[77] Strong adhesion to the Au substrate and enhanced electrochemical characteristics and durability of PEDOT films were achieved with the introduction of these double dopants. It was demonstrated that the PEDOT:PSS:MXene film exhibited exceptional mechanical and electrochemical stability together with high volumetric capacitance. Furthermore, the PEDOT:PSS:MXene electrode enhanced electrochemical activity toward DA in a linear range from 1 μM to 100 μM. Boobphahom *et al.* developed a hydrogel using a combination of titanium dioxide/MXene with polyvinyl alcohol/graphene oxide (TiO_2/MXene–PVA/GO) and this hydrogel was then used to modify a screen-printed carbon electrode (SPCE) to detect urinary norepinephrine (NE).[78] The

hydrophilic three-dimensional networks in the PVA/GO hydrogels result in excellent sample absorption, and combining them with TiO_2/MXene makes them an exciting modifier for electrochemical sensors for absorbent materials. The modified electrode offered comparable linear ranges with a low LOD value compared to earlier reports. Additionally, the linearity acquired from this sensor (1.0 and 60.0 μM) enables differentiation between healthy individuals (NE approximately 0.8 μM to 4.0 μM) and patients with possible neurological problems. The composite was also utilised for the detection of urine NE by integrating it into the panty liners of patients, enabling the early identification of neurological illnesses.

The application of MXene in immobilizing enzymes and creating biosensors needs additional research due to its exceptional features and distinctive structure. In line with this, Xia and his co-workers constructed a simple MXene-based enzymatic electrochemical biosensor by utilizing the beneficial properties of MXene and chitosan (Chit).[79] Chit and $Ti_3C_2T_x$ function as a support matrix to immobilise the cholesterol oxidase (ChOx) enzyme and improve electrical conductivity. A continuous self-assembling technique created the hierarchical accordion-like Chit/ChOx/$Ti_3C_2T_x$ nanocomposite for monitoring cholesterol by selectively oxidizing cholesterol to cholest-4-en-3-one and H_2O_2 (Fig. 8a). The Chit/ChOx/$Ti_3C_2T_x$ synthesized was demonstrated to have a porous structure, which helps in improving the effective surface area of the modified electrode (Fig. 8b). The electro-oxidation current was monitored using DPV with the formation of H_2O_2, the by-product of the ChOx process (Fig. 8c). Moreover, the suggested electrochemical technique has demonstrated outstanding stability and reproducibility for the detection of cholesterol in real samples.

Another type of enzymatic MXene-based sensor was developed by Hroncekova *et al.* using $Ti_3C_2T_x$ MXene and chitosan to detect sarcosine[80] (Fig. 8d). The 2D multilayered porous nanostructure of MXene-based layers (Fig. 8e) provides a great surface area for sarcosine oxidase (SOx) immobilization, and this leads to improved performance and sensitivity of the fabricated biosensor. Sarcosine was indirectly detected by amperometric measurement of H_2O_2 generated during the enzymatic process (Fig. 8f).[80] The modified GCE exhibited a linear range of up to 7.8 μM and a low detection limit of 18 nM. As a clinical application, the SOx/MXene–Chi/GCE device was applied to determine sarcosine in artificial urine samples. These two studies on

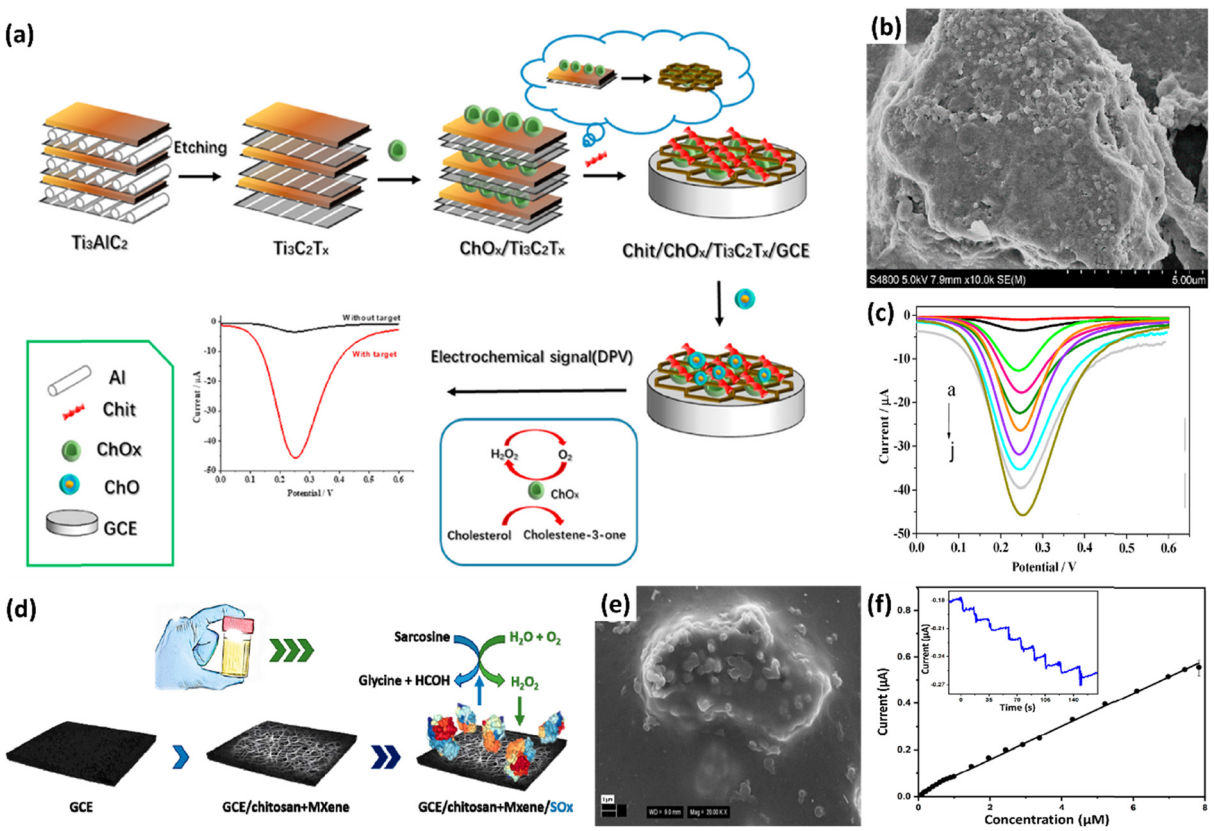

Fig. 8 (a) Schematic illustrations of a) Chit/ChOx/$Ti_3C_2T_x$/GCE development and the cholesterol reaction mechanism at the modified GCE. (b) SEM image of Chit/ChOx/$Ti_3C_2T_x$/GCE. c) DPV of the Chit/ChOx/$Ti_3C_2T_x$/GCE biosensor in different concentrations of cholesterol. (a to c) Reproduced with permission from ref. 79. Copyright (2021) Elsevier. d) MXene/chitosan nanocomposite modified GCE as a support for sarcosine oxidase (SOx) immobilisation and indirect sarcosine detection in urine, based on hydrogen peroxide electrochemical reduction. e) SEM image of the MXene/chitosan nanocomposite. f) Calibration plot of the SOx/MXene–Chi/GCE biosensor. Inset: Current *vs.* time response of the SOx/MXene–Chi/GCE biosensor. f) Reproduced with permission from ref. 80. Copyright (2020) Processes.

MXene–biopolymer-based composites demonstrate the effectiveness of MXene-based composites in health monitoring by demonstrating their ability to identify by-products produced during intricate biological processes. Similarly, the abundance of active terminations on the surface of MXenes enables the incorporation of a diverse range of polymers through *in situ* polymerisation or *ex situ* blending.[73,81–83] The exceptionally high dispersibility of MXene in water allows for its easy aqueous phase mixing with any water soluble polymers to fabricate an MXene/

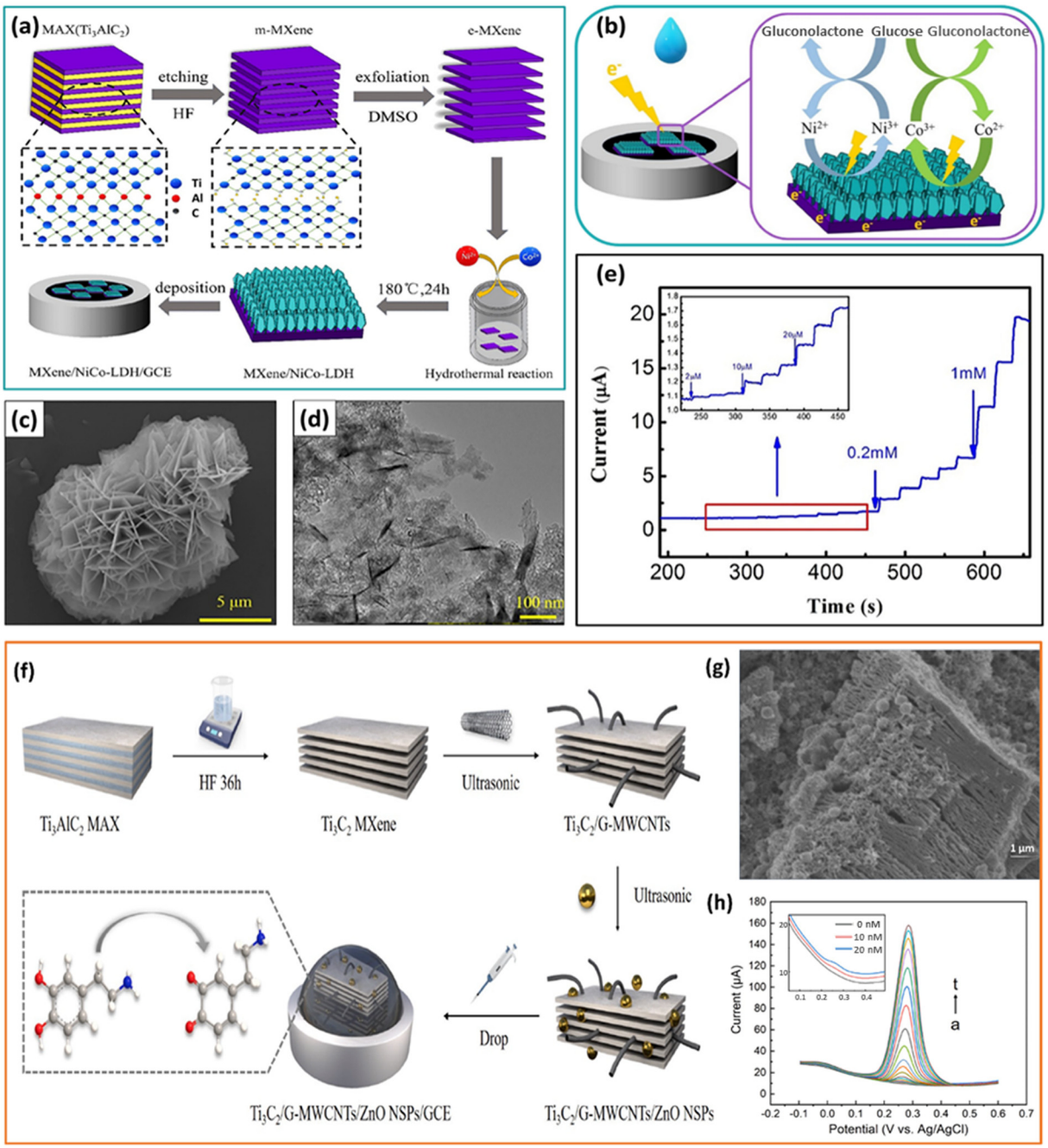

Fig. 9 a) Schematic representing the fabrication of MXene/NiCo-LDH/GCE. b) Illustration of the mechanism of the oxidation of glucose on the surface of MXene/NiCo-LDH/GCE in an alkaline solution. c) SEM image and (d) TEM image of the MXene/NiCo-LDH composite. e) The chronoamperometry curve of MXene/NiCo-LDH/GCE obtained by successive addition of different concentrations of glucose into the electrolyte every 25 s; inset: magnified image of the marked region in the chronoamperometry curve. (a to e) Reproduced with permission from ref. 55. Copyright (2019) Elsevier. f) Illustration of the synthesis and fabrication of Ti_3C_2/G-MWCNTs/ZnO/GCE for detection of DA. g) SEM image of Ti_3C_2/G-MWCNTs/ZnO. h) DPVs of DA quantitative analysis on Ti_3C_2/G-MWCNTs/ZnO/GCE at various concentrations of DA (a to t: 0, 0.01, 0.02, 0.04, 0.08, 0.12, 0.2, 0.3, 0.5, 0.8, 1.2, 2, 3, 5, 7, 10, 15, 20, 25, 30 μM); inset: the magnified image of the DPV plot in the concentration range 0, 10, and 20 nM. (f to h) Reproduced with permission from ref. 86. Copyright (2022) Elsevier.

polymer nanocomposite sensor. Furthermore, polymers can not only enhance the required electrochemical response but also prevent the oxidation of MXene.[84] Optimal blending of polymers results in the creation of a three-dimensional network of conductive nanosheets, which in turn aids in the production of electrochemical sensors.

3.6 Other MXene–hybrid nanocomposites as electrochemical sensors

Hybridization of MXenes with various electroactive materials is crucial in enhancing the performance of electrochemical sensors. For the first time, nickel–cobalt layered double hydroxide (NiCo-LDH) nanosheets were synthesised on the surface of Ti_3C_2 MXene using a simple hydrothermal technique, generating three-dimensional porous MXene/NiCo-LDH nanocomposites (Fig. 9a) that are potentially employed for non-enzymatic glucose detection in real samples.[55] The process of glucose oxidation on the surface of NiCo-LDH in an alkaline solution begins with glucose deprotonation, followed by the simultaneous reduction of Ni(III) to Ni(II) and Co(III) to Co(II) (Fig. 9b). NiCo-LDH nanosheets grow vertically on the surface of MXene to generate a 3D porous structure with a large specific surface area (Fig. 9c and d) and additional ion transport channels, offering easy glucose access for electrochemical processes. Due to the outstanding conductivity of the MXene substrate and the 3D porous structure of the composite, the electron transfer rate is boosted compared to NiCo-LDH. Chronoamperometric examinations were performed to detect glucose (Fig. 9e), and the composite proved to be a promising option for non-enzymatic glucose sensing with a wide linearity range, low detection limit, and rapid response. In another work, Alanazi *et al.* proposed a method to fabricate a non-enzymatic glucose sensor by building Cu_2O on the 3D porous structures of MXene sheets and rGO.[85] Here, the biosensing catalyst Cu_2O was added by a coprecipitation technique to a 3D binary composite of MXene and rGO nanosheets synthesised by the hydrothermal process to form MXene/graphene aerogel/Cu_2O composites. A chronoamperometric study was carried out to understand the sensing performance of the composite. The fabricated electrode showed a detection limit of 1.1 μM and two wide linear ranges of 0.1–14 and 15–40 mM, respectively. These findings demonstrate that, in comparison to a 2D arrangement of MXene and rGO in a ternary composite, a 3D structure composed of assembled MXene and rGO will aid in efficient charge transfer and enhance the sensing activity of the non-enzymatic glucose sensor.

Owing to their inherent negative charges, MXenes can absorb cations and serve as nucleation sites for the growth of nanostructures.[87] Zheng *et al.* used MXene/DNA/Pd/Pt nanocomposites for the detection of DA, where the negatively charged phosphate backbone of the DNA and the metal ions interact electrostatically to produce MXene/DNA/Pd/Pt nanocomposites.[88] The adsorption of DNA on the surface of MXene nanosheets through π–π stacking interaction and successive deposition of Pd/Pt nanoparticles enhances the electrocatalytic activity towards DA. The developed sensor also demonstrated an outstanding response toward DA in human serum samples. Zhao *et al.* developed a multifunctional 3D carbon fibre paper–MXene–MoS_2 (CMM) sensing interface for the highly sensitive detection of several biomolecules (AA, DA, UA, and microRNA).[89] The unique array structure of the flexible CMM interface promotes the local enrichment of molecules, which improves the ultra-sensitive detection of biomolecules from complex fluids. Using the DPV technique, the CMM electrode was used for the simultaneous detection of AA, DA, and UA with an LOD of 0.89 μM, 0.23 μM, and 0.35 μM, respectively. Furthermore, the modified sensor also exhibited an ultra-high sensitivity of 3.16 aM towards the detection of miRNA. Dang *et al.* investigated Prussian blue (PB) nanoparticle intercalated Ti_3C_2 nanosheets (PB NPs/Ti_3C_2) for the non-enzymatic electrochemical detection of H_2O_2 released from living cells.[90] The synergistic effect between PB and Ti_3C_2 on the structure and performance optimization was connected with the outstanding electrochemical determination performance of PB/Ti_3C_2/GCE. The Ti_3C_2 layers coated with PB NPs had greater interlayer spacing and prevented PB NP accumulation, increasing the specific surface area and apparent exposure of active sites. Additionally, the two-dimensionally layered Ti_3C_2 and PB NPs provided shorter diffusion paths for the electrolyte and H_2O_2, facilitating the migration of electrons and ions and, in turn, increasing the reduction process of H_2O_2 on the PB/Ti_3C_2 surface. The human cervical cancer cells (HeLa) injected with *N*-formylmethionyl-leucyl-phenylalanine (fMLP), a stimulant to destroy cancer cells, were used for real-time analysis to produce H_2O_2. The current response of PB/Ti_3C_2/GCE during the successive injection of fMLP in the presence and absence of HeLa cells confirmed that H_2O_2 was produced from the living tumour cells. Amara *et al.* designed a composite material of perylene diimide (PDI) and MXene ($Ti_3C_2T_x$) for the electrochemical detection of DA.[91] The obtained composite was used to modify the graphitic pencil electrode to detect DA in the 100–1000 μM range with an LOD of 240 nM. PDI has been uniformly wrapped around MXene flakes *via* H bonding and π–π stacking. This powerful interaction creates a stable interface with several active DA adsorption sites, increasing electrochemical activity. The modified sensor also showed good responsiveness in human serum samples. Niamsi *et al.* fabricated a paper-based screen-printed ionic liquid/graphene electrode (SPIL–GE) modified with $Ti_3C_2T_x$, PB, glucose oxidase (GOx), and Nafion for the electrochemical detection of glucose.[92] An electrode was created for the first time using ionic liquid and graphene ink on a paper substrate. The performance of the SPIL–GE modified with PB/$Ti_3C_2T_x$/GOx/Nafion was examined using CV and chronoamperometry (CA) techniques. The prepared paper-based PB/$Ti_3C_2T_x$/GOx/Nafion/SPIL–GE was also used to measure blood glucose concentration for real sample analysis.

By taking advantage of the affordable non-metal doping, Chen *et al.* developed a structure with co-doped nitrogen (N) and sulphur (S) using thiourea as the doping source on

the surface of Ti_3C_2 nanosheets (NS-Ti_3C_2) to detect uric acid (UA).[93] The composite NS-Ti_3C_2 was synthesised using a simple one-step synthesis process, which produced more active sites due to the doping of N and S atoms, enhancing electron transport even further. A sensitive colourimetric method was also proposed to detect UA. The sensor achieved a linear range of 2–400 μM with a LOD of 0.19 μM and also detected UA in fresh serum samples. MXene and CNTs with superior electronic conductivity can be further hybridised with Cu-MOF to improve their poor conductivity. As a result, Chen *et al.* synthesised MXene/CNTs/Cu-MOF composites to imprint them on glassy carbon electrodes and to detect tyrosine.[94] Cu-MOF also has a high degree of porosity, which can be used to adsorb analyte molecules and enhance the detection signal in human serum with a high recovery rate. M. Ni *et al.* used ZnO nanospheres to improve the electrochemical activity of Ti_3C_2–graphitised multi-walled carbon nanotube composites (Ti_3C_2/G-MWCNTs) for the detection of DA[86] (Fig. 9f). The composite exhibits a decorated structure, which denotes excellent synergy between the three materials (Fig. 9g). Due to the unique features of the as-synthesised nanocomposite, such as fast electron transfer, good electrocatalytic performance, and excellent electrochemical activity, the sensor exhibits high sensitivity and detection performance for DA (Fig. 9h). A wide linear range (0.01–30 μM) with a low detection limit (3.2 nM) was achieved, and the sensor successfully detected DA in human serum samples. Assembly of versatile materials with 2D MXenes enables combinations of properties that no single material can provide and also

Table 1 Summary of MXene nanocomposite electrochemical sensors for detection of clinically relevant biomarkers

Nanocomposite category	Working electrode	Analyte	Analytical method	Limit of detection	Linear range	Real sample	Ref.
MXene–metal	Tri-AgNP/L-Cys/$Ti_3C_2T_x$	5-HT	DPV	0.08 μM	0.5–150 μM	Serum	58
	AuNP@Ti_3C_2	5hmC	CV	6.32×10^{-7} μM	6.32×10^{-7}–6.32×10^{-5} μM	Tumour cells	59
	AuNP@ $Ti_3C_2T_x$	UA, FA	Amperometry	0.0115 μM (UA) and 0.0062 μM (FA)	0.03–1520 μM (UA) and 0.02–3580 μM (FA)	Serum	60
	AuNPs/Ti_3C_2	miRNA-155	DPV	3.5×10^{-10} μM	1×10^{-9}–0.01 μM	—	61
	Pd/$Ti_3C_2T_x$	L-Cys	Amperometry	0.14 μM	0.5–10 μM	Urine	41
MXene–metal oxide	MXene/Co_3O_4	H_2O_2	LSV	0.5 μM	0–75 μM	Cancer cell	63
	SnO_2 QD@Ti_3C_2	DA	CV	0.002 μM	0.004–8.0 μM	Serum and urine	65
MXene–MOF	$Ti_3C_2T_x$/ZIF-67	Glucose	Amperometry	3.81 μM	5–7500 μM	—	48
	Ce-MOF/$Ti_3C_2T_x$	L-Trp	DPV	0.19 μM	0.2–139 μM	Blood serum	66
	MOF–Ti_3C_2	DA	DPV	0.11 μM	0.09–0.13 μM	Blood serum	47
MXene–carbon	$Ti_3C_2T_x$–rGO	Serotonin	DPV	0.01 μM	0.025–147 μM	Blood plasma	68
	MXene–graphene	Nicotine	DPV and amperometry	0.29 μM and 2.8×10^{-4} μM	1–55 μM and 0.03–0.6 μM	Saliva	69
	$Ti_3C_2T_x$/N-rGO	AD	DPV	0.003 μM	0.01–90.0 μM	Urine	50
	$Ti_3C_2T_x$/rGO	EP	DPV	0.0035 μM	1–60 μM	Urine	71
	MXene@ PDA/NH_2-MWCNTs	AAP	DPV	0.001 μM	0.005–60 μM	Urine	72
MXene–polymer	$Ti_3C_2T_x$/PPy	DA and UA	DPV	0.37 μM (DA), 0.15 μM (UA)	12.5–125 μM (DA), 50–500 μM (UA)	—	76
	PEDOT:PSS:MXene	DA	DPV	—	1–100 μM	—	77
	TiO_2/MXene–PVA/GO	NE	Amperometry	0.008 μM	0.01–60.0 μM	Urine	78
	Chit/ChOx/$Ti_3C_2T_x$	Cholesterol	DPV	1.1×10^{-4} μM	0.0003–0.0045 μM	Serum	79
	SOx/MXene–Chi	Sarcosine	CA	0.018 μM	0.036–7.8 μM	Urine	80
Other MXene hybrid materials	MXene/NiCo-LDH	Glucose	CA	0.53 μM	2–4096 μM	Serum	55
	MXene/graphene aerogel/Cu_2O	Glucose	CA	1.1 μM	100–1.4×10^4 and 1.5×10^4–4×10^4 μM	Serum	85
	Ti_3C_2/DNA/Pd/Pt	DA	Amperometry	0.03 μM	0.2–1000 μM	Serum	88
	Carbon fiber paper–MXene–MoS_2	AA, DA, UA and miRNA	DPV	0.89 μM (AA), 0.23 μM (DA), and 0.35 μM (UA), miRNA (3.16×10^{-12} μM)	—	Serum and urine	89
	PB NPs/Ti_3C_2	H_2O_2	Amperometry	0.20 μM	0.60–63.6 μM and 63.6–254 μM	HeLa cells	90
	PDI–MXene	DA	Amperometry	0.24 μM	100–1000 μM	Serum	91
	PB/$Ti_3C_2T_x$/GOx/Nafion	Glucose	CA	24 μM	80–1.5×10^4 μM	Blood	92
	NS-Ti_3C_2 nanosheets	UA	CV	0.19 μM	2–400 μM	Serum	93
	MXene/CNT/CuMOF	Tyrosine	DPV	0.19 μM	0.53–232.46 μM	Serum	94
	Ti_3C_2/G-MWCNT/ZnO	DA	DPV	0.0032 μM	0.01–30 μM	Serum	86

create a wide range of heterostructures or ordered structures, thereby promoting the emergence of high-performance next generation devices. Table 1 consolidates recent reports on various MXene-based electrocatalytically active nanocomposites for the detection of clinically relevant biomarkers for diagnostic applications in various body fluids.

4. Conclusions and future perspectives

MXenes are promising for electrochemical applications because of their remarkable surface terminal functional groups, 2D structure, stability, good electrical conductivity, and processability. However, self-stacking and easy oxidation of MXenes significantly limit their employability for potential applications. A pressing challenge in fabricating MXene-based electrodes is to avoid self-restacking while maintaining the outstanding electrical conductivity and electrochemical activity of MXenes. MXene, in conjunction with other materials, may overcome the fallbacks of pristine MXene and is suggested to broaden its pertinency in applications ranging from sustainable energy technologies to point-of-care diagnostics. Hybridisation of nanostructures with 2D MXenes enables the tuning of their physical, chemical, and electrochemical properties by combining the best qualities of each component and even bringing about synergistic effects. Compared to pristine MXenes, MXene-based composites show better peak current, reproducibility, and stability due to the large specific surface area and the electroactive sites of MXene in the composites. In addition, during the fabrication of nanocomposites, the spacers that can be evenly inserted into MXene nanosheets will have more practical significance in improving the electrochemical performance. Consequently, chemical modification of MXene using modifiers that can intercalate into the interlayers rather than mostly attaching to surfaces will be an attractive choice for synthesizing hybrid nanomaterials with better electrocatalytic performance and conductivity.

Plenty of research on the development of various types of electrochemical sensors has been conducted since the discovery of MXene. However, the bulk of studies have remained focused on titanium carbide ($Ti_3C_2T_x$ materials)[95] owing to its excellent metallic conductivity and stability across a wide temperature range. Among all MXenes, Ti_3C_2 shows prominent conductivity and large active surface area for effective immobilization in view of constructing mediator-free biosensors. Moreover, exceptional hydrophilicity of Ti_3C_2-MXene confers biocompatibility, making it an excellent material for the development of electrochemical sensors that can detect biomolecules.[96] Thus, Ti_3C_2-MXene has demonstrated potential for use in all fields involving sensitive biomarker detection with a broad linear range and low detection limit. In this review, we mainly focused on $Ti_3C_2T_x$, the most researched 2D MXene, and its composites developed for health monitoring. This review initially focused on the hybridization of $Ti_3C_2T_x$ MXene with electroactive materials such as carbon nanomaterials, metals, metal oxides, and polymers. Successively, the practical viability of the nanocomposites toward the detection of various biomarkers from complex biological fluids has been reviewed. We present a thorough categorisation and analysis of different MXene-based nanocomposites, highlighting their structural–property correlation and underscoring the influence of MXenes on the improved electrochemical performance.

However, the study of electrochemical sensors based on MXenes is still in its early phases, more focus is needed for their development and employment in real-life problems. The conductive structure, sensing mechanism, and sensor performance of MXenes have facilitated their progressive integration into the field of electrochemical sensing. By carefully evaluating the benefits of MXenes and the specific sensing requirements, novel sensing composites can be developed by integrating MXenes with other appropriate materials. This approach aims to optimise the synergistic impact between MXenes and other phase materials, resulting in a high-performance sensor with exceptional sensitivity and a broad response range. Nevertheless, pristine MXenes are susceptible to extreme oxidation under normal environmental conditions, unlike other conductive low-dimensional nanomaterials and have poor stability in air, humidity or water media.[19] These constraints of pristine MXenes before compositing can be resolved to an extent by using proper storage conditions like an argon environment and exploiting non-aqueous solvents like ethanol, DMF, *etc.* Furthermore, a deeper understanding of the terminal groups of MXenes is highly essential as these groups and any related defects will significantly influence the electron transfer rates and hence sensor's operation. The fundamental understanding of the interaction of active molecules on the surface of MXenes is crucial in designing and synthesis of nanocomposites with enhanced electrochemical performance. Although several biocompatible MXene-based composites have been developed, additional research is still required to fully assess their toxicity and biosafety. As the detection of clinically relevant biomolecules is still in its infancy, there are still additional avenues concerning the simultaneous or individual transduction mechanisms of numerous clinically relevant biomarkers that require further investigation. Further investigation into the biofouling of neurotransmitter sensors in complex environments could potentially mitigate the logistical challenges associated with the creation of ubiquitous devices.

Data availability

No primary research results, software or code have been included and no new data were generated or analysed as part of this review.

Author contributions

The manuscript was written through the contributions of all authors. All authors have given approval to the final version of the manuscript.

Conflicts of interest

The authors declare no conflict of interest.

Acknowledgements

MMM greatly acknowledges the funding from the Science and Engineering Research Board (SERB) – POWER project (SPG/2021/004078) by the Department of Science and Technology (DST), India.

References

1 J. Baranwal, B. Barse, G. Gatto, G. Broncova and A. Kumar, Electrochemical Sensors and Their Applications: A Review, *Chemosensors*, 2022, **10**, 363.
2 Y. Wang, H. Xu, J. Zhang, G. Li, Y. Wang, H. Xu, J. Zhang and G. Li, Electrochemical sensors for clinic analysis, *Sensors*, 2008, **8**, 2043–2081.
3 U. Guth, W. Vonau and J. Zosel, Recent developments in electrochemical sensor application and technology - A review, *Meas. Sci. Technol.*, 2009, **20**, 042002.
4 R. Mayeux, Biomarkers: Potential Uses and Limitations, *NeuroRx*, 2004, **1**, 182–188.
5 M. Labib, E. H. Sargent and S. O. Kelley, Electrochemical Methods for the Analysis of Clinically Relevant Biomolecules, *Chem. Rev.*, 2016, **116**, 9001–9090.
6 D. Grieshaber, R. MacKenzie, J. Vörös and E. Reimhult, Electrochemical biosensors - Sensor principles and architectures, *Sensors*, 2008, **8**, 1400–1458.
7 O. Simoska and K. J. Stevenson, Electrochemical sensors for rapid diagnosis of pathogens in real time, *Analyst*, 2019, **144**, 6461–6478.
8 D. Tyagi, H. Wang, W. Huang, L. Hu, Y. Tang, Z. Guo, Z. Ouyang and H. Zhang, Recent advances in two-dimensional-material-based sensing technology toward health and environmental monitoring applications, *Nanoscale*, 2020, **12**, 3535–3559.
9 D. R. Thévenot, K. Toth, R. A. Durst and G. S. Wilson, Electrochemical biosensors: Recommended definitions and classification, *Anal. Lett.*, 2001, **34**, 635–659.
10 K. Beaver, A. Dantanarayana and S. D. Minteer, Materials Approaches for Improving Electrochemical Sensor Performance, *J. Phys. Chem. B*, 2021, **125**, 11820–11834.
11 Á. Terán-Alcocer, F. Bravo-Plascencia, C. Cevallos-Morillo and A. Palma-Cando, Electrochemical sensors based on conducting polymers for the aqueous detection of biologically relevant molecules, *Nanomaterials*, 2021, **11**, 1–62.
12 L. Karadurmus, S. I. Kaya, A. Cetinkaya and S. A. Ozkan, Trends in Analytical Chemistry New brand MXene-based electrochemical point-of-care sensors as novel diagnostic devices, *TrAC, Trends Anal. Chem.*, 2023, **165**, 117145.
13 M. Ankitha, A. M. Arjun, N. Shabana and P. A. Rasheed, A Mini Review on Recent Advances in MXene Based Electrochemical Wearable Sensing Devices, *Biomedical Materials & Devices*, 2022, **1**, 339–350.
14 M. A. Khan, F. Ramzan, M. Ali, M. Zubair, M. Q. Mehmood and Y. Massoud, Emerging Two-Dimensional Materials-Based Electrochemical Sensors for Human Health and Environment Applications, *Nanomaterials*, 2023, **13**, 780.
15 K. Xie, J. Wang, S. Xu, W. Hao, L. Zhao, L. Huang and Z. Wei, Application of Two-Dimensional MXene materials in sensors, *Mater. Des.*, 2023, **228**, 111867.
16 M. Naguib, O. Mashtalir, J. Carle, V. Presser, J. Lu, L. Hultman, Y. Gogotsi and M. W. Barsoum, Two-dimensional transition metal carbides, *ACS Nano*, 2012, **6**, 1322–1331.
17 A. V. Mohammadi, J. Rosen and Y. Gogotsi, The world of two-dimensional carbides and nitrides (MXenes), *Science*, 2021, **372**, 6547.
18 M. Alhabeb, K. Maleski, B. Anasori, P. Lelyukh, L. Clark, S. Sin and Y. Gogotsi, Guidelines for Synthesis and Processing of Two-Dimensional Titanium Carbide ($Ti_3C_2T_x$ MXene), *Chem. Mater.*, 2017, **29**, 7633–7644.
19 M. Shekhirev, C. E. Shuck, A. Sarycheva and Y. Gogotsi, Safe Synthesis of MAX and MXene: Guidelines to Reduce Risk during Synthesis, *Prog. Mater. Sci.*, 2021, **120**, 1–31.
20 B. Anasori, M. Lukatskaya and Y. Gogotsi, 2D metal carbides and nitrides (MXenes) for energy storage, *Nat. Rev. Mater.*, 2017, **2**, 16098.
21 B. Anasori and Y. Gogotsi, *2D Metal carbides and nitrides (MXenes): Structure, properties and applications*, 2019.
22 H. Lin, X. Wang, L. Yu, Y. Chen and J. Shi, Two-Dimensional Ultrathin MXene Ceramic Nanosheets for Photothermal Conversion, *Nano Lett.*, 2017, **17**, 384–391.
23 C. Dai, H. Lin, G. Xu, Z. Liu, R. Wu and Y. Chen, Biocompatible 2D Titanium Carbide (MXenes) Composite Nanosheets for pH-Responsive MRI-Guided Tumor Hyperthermia, *Chem. Mater.*, 2017, **29**, 8637–8652.
24 U. Amara, I. Hussain, M. Ahmad, K. Mahmood and K. Zhang, 2D MXene-Based Biosensing: A Review, *Small*, 2023, **19**, 2205249.
25 A. Rhouati, M. Berkani, Y. Vasseghian and N. Golzadeh, MXene-based electrochemical sensors for detection of environmental pollutants: A comprehensive review, *Chemosphere*, 2022, **291**, 132921.
26 F. Ezzah Ab Latif, A. Numan, N. M. Mubarak, M. Khalid, E. C. Abdullah, N. A. Manaf and R. Walvekar, Evolution of MXene and its 2D heterostructure in electrochemical sensor applications, *Coord. Chem. Rev.*, 2022, **471**, 214755.
27 Z. U. D. Babar, B. Della Ventura, R. Velotta and V. Iannotti, Advances and emerging challenges in MXenes and their nanocomposites for biosensing applications, *RSC Adv.*, 2022, **12**, 19590–19610.
28 H. Weng, A. Ranjbar, Y. Liang, Z. Song, M. Khazaei, S. Yunoki, M. Arai, Y. Kawazoe, Z. Fang and X. Dai, Large-gap two-dimensional topological insulator in oxygen

functionalized MXene, *Phys. Rev. B: Condens. Matter Mater. Phys.*, 2015, **92**, 1–7.

29 F. Wang, C. Yang, C. Duan, D. Xiao, Y. Tang and J. Zhu, An Organ-Like Titanium Carbide Material (MXene) with Multilayer Structure Encapsulating Hemoglobin for a Mediator-Free Biosensor, *J. Electrochem. Soc.*, 2015, **162**, B16–B21.

30 F. Shahzad, A. Iqbal, S. A. Zaidi, S. W. Hwang and C. M. Koo, Nafion-stabilized two-dimensional transition metal carbide (MXene) as a high-performance electrochemical sensor for neurotransmitter, *J. Ind. Eng. Chem.*, 2019, **79**, 338–344.

31 P. V. Vaishag, S. A. Mohandas, M. Mufeeda, P. Gangadharan and P. A. Rasheed, Conversion of electronic waste to an electrochemical sensor for dopamine: Using MXene-modified liquid crystal display panels, *ACS Sustainable Chem. Eng.*, 2023, **11**, 12771–12779.

32 M. Ashton, K. Mathew, R. G. Hennig and S. B. Sinnott, Predicted Surface Composition and Thermodynamic Stability of MXenes in Solution, *J. Phys. Chem. C*, 2016, **120**, 3550–3556.

33 K. Maleski, V. N. Mochalin and Y. Gogotsi, Dispersions of Two-Dimensional Titanium Carbide MXene in Organic Solvents, *Chem. Mater.*, 2017, **29**, 1632–1640.

34 X. Wu, P. Ma, Y. Sun, F. Du, D. Song and G. Xu, Application of MXene in Electrochemical Sensors: A Review, *Electroanalysis*, 2021, **33**, 1827–1851.

35 L. Gao, W. Bao, A. V. Kuklin, S. Mei, H. Zhang and H. Ågren, Hetero-MXenes: Theory, Synthesis, and Emerging Applications, *Adv. Mater.*, 2021, **33**, 2004129.

36 C. Wang, S. Chen and L. Song, Tuning 2D MXenes by Surface Controlling and Interlayer Engineering: Methods, Properties, and Synchrotron Radiation Characterizations, *Adv. Funct. Mater.*, 2020, **30**, 2000869.

37 M. Naguib, V. N. Mochalin, M. W. Barsoum and Y. Gogotsi, 25th Anniversary Article: MXenes: A New Family of Two-Dimensional Materials, *Adv. Mater.*, 2014, **26**, 992–1005.

38 M. Naguib, M. W. Barsoum and Y. Gogotsi, Ten Years of Progress in the Synthesis and Development of MXenes, *Adv. Mater.*, 2021, **33**, 1–10.

39 M. Pershaanaa, F. Kamarulazam, O. Gerard, Z. L. Goh, S. Bashir, K. Baruah, P. Deb, S. Ramesh and K. Ramesh, MXenes and their transformation to composites for potential applications, *Mater. Today Commun.*, 2023, **35**, 106143.

40 H. Aghamohammadi, R. Eslami-Farsani and E. Castillo-Martinez, Recent trends in the development of MXenes and MXene-based composites as anode materials for Li-ion batteries, *J. Energy Storage*, 2022, **47**, 103572.

41 P. A. Rasheed, R. P. Pandey, K. A. Jabbar, J. Ponraj and K. A. Mahmoud, Sensitive electrochemical detection of l-cysteine based on a highly stable Pd@$Ti_3C_2T_X$(MXene) nanocomposite modified glassy carbon electrode, *Anal. Methods*, 2019, **11**, 3851–3856.

42 L. Lorencova, T. Bertok, J. Filip, M. Jerigova, D. Velic, P. Kasak, K. A. Mahmoud and J. Tkac, Highly stable $Ti_3C_2T_x$ (MXene)/Pt nanoparticles-modified glassy carbon electrode for H_2O_2 and small molecules sensing applications, *Sens. Actuators, B*, 2018, **263**, 360–368.

43 R. Zhang, J. Liu and Y. Li, MXene with Great Adsorption Ability toward Organic Dye: An Excellent Material for Constructing a Ratiometric Electrochemical Sensing Platform, *ACS Sens.*, 2019, **4**, 2058–2064.

44 Y. T. Liu, P. Zhang, N. Sun, B. Anasori, Q. Z. Zhu, H. Liu, Y. Gogotsi and B. Xu, Self-Assembly of Transition Metal Oxide Nanostructures on MXene Nanosheets for Fast and Stable Lithium Storage, *Adv. Mater.*, 2018, **30**, 1707334.

45 L. P. Yu, X. H. Zhou, L. Lu, L. Xu and F. J. Wang, MXene/Carbon Nanotube Hybrids: Synthesis, Structures, Properties, and Applications, *ChemSusChem*, 2021, **14**, 5079.

46 A. Zarepour, S. Ahmadi, N. Rabiee and A. Zarrabi, Self-Healing MXene and Graphene-Based Composites: Properties and Applications, *Nano-Micro Lett.*, 2023, **15**, 1–28.

47 J. Paul and J. Kim, Reticular synthesis of a conductive composite derived from metal-organic framework and Mxene for the electrochemical detection of dopamine, *Appl. Surf. Sci.*, 2023, **613**, 156103.

48 X. Han, K. Cao, Y. Yao, J. Zhao, C. Chai and P. Dai, A novel electrochemical sensor for glucose detection based on a $Ti_3C_2T_x$/ZIF-67 nanocomposite, *RSC Adv.*, 2022, **12**, 20138–20146.

49 Y. Liu, J. Yu, D. Guo, Z. Li and Y. Su, $Ti_3C_2T_x$ MXene/graphene nanocomposites: Synthesis and application in electrochemical energy storage, *J. Alloys Compd.*, 2020, **815**, 152403.

50 S. Chen, M. Shi, Q. Xu, J. Xu and X. Duan, $Ti_3C_2T_x$ MXene/nitrogen-doped reduced graphene oxide composite: a high-performance electrochemical sensing platform for adrenaline detection, *Nanotechnology*, 2021, **32**, 265501.

51 M. Carey and M. W. Barsoum, MXene polymer nanocomposites: a review, *Mater. Today Adv.*, 2021, **9**, 100120.

52 Y. Gogotsi and Q. Huang, MXenes: Two-Dimensional Building Blocks for Future Materials and Devices, *ACS Nano*, 2021, **15**, 5775–5780.

53 H. Chang, X. Li, L. Shi, Y. R. Zhu and T. F. Yi, Towards high-performance electrocatalysts and photocatalysts: Design and construction of MXenes-based nanocomposites for water splitting, *Chem. Eng. J.*, 2021, **421**, 129944.

54 Z. Ling, C. E. Ren, M. Q. Zhao, J. Yang, J. M. Giammarco, J. Qiu, M. W. Barsoum and Y. Gogotsi, Flexible and conductive MXene films and nanocomposites with high capacitance, *Proc. Natl. Acad. Sci. U. S. A.*, 2014, **111**, 16676–16681.

55 M. Li, L. Fang, H. Zhou, F. Wu, Y. Lu, H. Luo, Y. Zhang and B. Hu, Three-dimensional porous MXene/NiCo-LDH composite for high performance non-enzymatic glucose sensor, *Appl. Surf. Sci.*, 2019, **495**, 143554.

56 S. H. W. Kok, J. Lee, L. L. Tan, W. J. Ong and S. P. Chai, MXene - A New Paradigm Toward Artificial Nitrogen Fixation for Sustainable Ammonia Generation: Synthesis, Properties, and Future Outlook, *ACS Mater. Lett.*, 2022, **4**, 212–245.

57 X. Tu, F. Gao, X. Ma, J. Zou, Y. Yu, M. Li, F. Qu, X. Huang and L. Lu, MXene/carbon nanohorn/β-cyclodextrin-Metal-organic frameworks as high-performance electrochemical

sensing platform for sensitive detection of carbendazim pesticide, *J. Hazard. Mater.*, 2020, **396**, 122776.

58 J. Chen, S. Li, Y. Chen, J. Yang, J. Dong and X. Lu, L-Cysteine-Terminated Triangular Silver Nanoplates/MXene Nanosheets are Used as Electrochemical Biosensors for Efficiently Detecting 5-Hydroxytryptamine, *Anal. Chem.*, 2021, **93**, 16655–16663.

59 K. Sideeq, S. Byun, A. Alam, M. Ko, J. An and S. Lim, A fast and label-free detection of hydroxymethylated DNA using a nozzle-jet printed AuNPs@Ti_3C_2 MXene-based electrochemical sensor, *Talanta*, 2022, **244**, 123421.

60 S. Elumalai, V. Mani, N. Jeromiyas, V. K. Ponnusamy and M. Yoshimura, A composite film prepared from titanium carbide $Ti_3C_2T_x$ (MXene) and gold nanoparticles for voltammetric determination of uric acid and folic acid, *Microchim. Acta*, 2020, **187**, 33.

61 X. Yang, M. Feng, J. Xia, F. Zhang and Z. Wang, An electrochemical biosensor based on AuNPs/Ti_3C_2 MXene three-dimensional nanocomposite for microRNA-155 detection by exonuclease III-aided cascade target recycling, *J. Electroanal. Chem.*, 2020, **878**, 114669.

62 L. Lorencova, T. Bertok, E. Dosekova, A. Holazova, D. Paprckova, A. Vikartovska, V. Sasinkova, J. Filip, P. Kasak, M. Jerigova, D. Velic, K. A. Mahmoud and J. Tkac, Electrochemical performance of $Ti_3C_2T_x$ MXene in aqueous media: towards ultrasensitive H_2O_2 sensing, *Electrochim. Acta*, 2017, **235**, 471–479.

63 S. Singh, A. Numan, M. Khalid, I. Bello, E. Panza and S. Cint, Facile and Affordable Design of MXene-Co_3O_4-Based Nanocomposites for Detection of Hydrogen Peroxide inCancer Cells: Toward Portable Tool for Cancer Management, *Small*, 2023, **19**, 2208209.

64 C. Burda, X. Chen, R. Narayanan and M. A. El-sayed, Chemistry and Properties of Nanocrystals of Different Shapes, *Chem. Rev.*, 2005, **105**, 1025–1102.

65 Y. Shi, K. Hu, L. Mei, X. Yang, Y. Shi, X. Wu, X. Min Li, M. Miao and S. Zhang, SnO_2 quantum dots-functionalized Ti_3C_2 MXene nanosheets for electrochemical determination of dopamine in body fluids, *Microchim. Acta*, 2022, **189**, 1–10.

66 Y. Chen, S. Li, L. Zhang, T. Jing, J. Wang, L. Zhao, F. Li, C. Li and J. Sun, Facile and fast synthesis of three-dimensional Ce-MOF/$Ti_3C_2T_X$ MXene composite for high performance electrochemical sensing of L-Tryptophan, *J. Solid State Chem.*, 2022, **308**, 122919.

67 J. Jyoti, B. P. Singh, M. Sandhu and S. K. Tripathi, Energy & Fuels materials for lithium-ion batteries, *Sustainable Energy Fuels*, 2022, **6**, 971–1013.

68 M. Su, H. Lan, L. Tian, M. Jiang, X. Cao, C. Zhu and C. Yu, $Ti_3C_2T_x$-reduced graphene oxide nanocomposite-based electrochemical sensor for serotonin in human biofluids, *Sens. Actuators, B*, 2022, **367**, 132019.

69 J. Rajendran, A. K. Sundramoorthy, D. Ganapathy, R. Atchudan, M. A. Habila and D. Nallaswamy, 2D MXene/graphene nanocomposite preparation and its electrochemical performance towards the identification of nicotine level in human saliva, *J. Hazard. Mater.*, 2022, **440**, 129705.

70 J. K. Wychowaniec, J. Litowczenko, K. Tadyszak, V. Natu, C. Aparicio, B. Pepli, M. W. Barsoum and M. Otyepka, Unique cellular network formation guided by heterostructures based on re duce d graphene oxide - $Ti_3C_2T_x$ MXene hydrogels, *Acta Biomater.*, 2020, **115**, 104–115.

71 Z. Li, Y. Guo, H. Yue, X. Gao, S. Huang, X. Zhang, Y. Yu, H. Zhang and H. Zhang, Electrochemical determination of epinephrine based on $Ti_3C_2T_x$ MXene-reduced graphene oxide/ITO electrode, *J. Electroanal. Chem.*, 2021, **895**, 115425.

72 S. Chen, J. Xu, M. Shi, Y. Yu, Q. Xu, X. Duan, Y. Gao and L. Lu, Polydopamine bridged MXene and NH_2-MWCNTs nanohybrid for high-performance electrochemical sensing of Acetaminophen, *Appl. Surf. Sci.*, 2021, **570**, 151149.

73 S. He, X. Sun, H. Zhang, C. Yuan, Y. Wei and J. Li, Preparation Strategies and Applications of MXene-Polymer Composites: A Review, *Macromol. Rapid Commun.*, 2021, **42**(19), 2100324.

74 G. Monastyreckis, L. Mishnaevsky, C. B. Hatter, A. Aniskevich, Y. Gogotsi and D. Zeleniakiene, Micromechanical modeling of MXene-polymer composites, *Carbon*, 2020, **162**, 402–409.

75 J. Li, X. Li and B. Van Der Bruggen, An MXene-based membrane for molecular separation, *Environ. Sci.: Nano*, 2020, **7**, 1289–1304.

76 Q. You, Z. Guo, R. Zhang, Z. Chang, M. Ge, Q. Mei and W. Dong, Simultaneous recognition of dopamine and uric acid in the presence of ascorbic acid via an intercalated mxene/ppy nanocomposite, *Sensors*, 2021, **21**, 3069.

77 S. Wustoni, A. Saleh, J. K. El-Demellawi, A. Koklu, A. Hama, V. Druet, N. Wehbe, Y. Zhang and S. Inal, MXene improves the stability and electrochemical performance of electropolymerized PEDOT films, *APL Mater.*, 2020, **8**, 121105.

78 S. Boobphahom, T. Siripongpreda, D. D. Zhang, J. Qin, P. Rattanawaleedirojn and N. Rodthongkum, TiO_2/MXene-PVA/GO hydrogel-based electrochemical sensor for neurological disorder screening via urinary norepinephrine detection, *Microchim. Acta*, 2021, **188**, 387.

79 T. Xia, G. Liu, J. Wang, S. Hou and S. Hou, MXene-based enzymatic sensor for highly sensitive and selective detection of cholesterol, *Biosens. Bioelectron.*, 2021, **183**, 113243.

80 S. Hroncekova, T. Bertok, M. Hires, E. Jane, L. Lorencova, A. Vikartovska, A. Tanvir, P. Kasak and J. Tkac, Ultrasensitive $Ti_3C_2T_X$ MXene/chitosan nanocomposite-based amperometric biosensor for detection of potential prostate cancer marker in urine samples, *Processes*, 2020, **8**, 580.

81 X. Wang, D. Zhang, H. Zhang, L. Gong, Y. Yang, W. Zhao, S. Yu, Y. Yin and D. Sun, In situ polymerized polyaniline/MXene (V2C) as building blocks of supercapacitor and ammonia sensor self-powered by electromagnetic-triboelectric hybrid generator, *Nano Energy*, 2021, **88**, 106242.

82 X. Chen, Y. Zhao, L. Li, Y. Wang, J. Wang, J. Xiong, S. Du, P. Zhang, X. Shi and J. Yu, MXene/Polymer Nanocomposites: Preparation, Properties, and Applications, *Polym. Rev.*, 2021, **61**, 80–115.

83 H. Aghamohammadi, N. Amousa and R. Eslami-Farsani, Recent advances in developing the MXene/polymer nanocomposites with multiple properties: A review study, *Synth. Met.*, 2020, **273**, 116695.

84 Q. Guo, X. Zhang, F. Zhao, Q. Song, G. Su, Y. Tan, Q. Tao, T. Zhou, Y. Yu, Z. Zhou and C. Lu, Protein-Inspired Self-Healable Ti_3C_2 MXenes/Rubber-Based Supramolecular Elastomer for Intelligent Sensing, *ACS Nano*, 2020, **14**, 2788–2797.

85 N. Alanazi, T. S. Gopal, M. Muthuramamoorthy, A. A. E. Alobaidi, R. A. Alsaigh, M. H. Aldosary, S. Pandiaraj, M. Almutairi, A. N. Grace and A. Alodhayb, Cu_2O/MXene/rGO Ternary Nanocomposites as Sensing Electrodes for Nonenzymatic Glucose Sensors, *ACS Appl. Nano Mater.*, 2023, **6**, 12271–12281.

86 M. Ni, J. Chen, C. Wang, Y. Wang, L. Huang, W. Xiong, P. Zhao, Y. Xie and J. Fei, A high-sensitive dopamine electrochemical sensor based on multilayer Ti_3C_2 MXene, graphitized multi-walled carbon nanotubes and ZnO nanospheres, *Microchem. J.*, 2022, **178**, 107410.

87 A. Sinha, Dhanjai, H. Zhao, Y. Huang, X. Lu, J. Chen and R. Jain, MXene: An emerging material for sensing and biosensing, *TrAC, Trends Anal. Chem.*, 2018, **105**, 424–435.

88 J. Zheng, B. Wang, A. Ding, B. Weng and J. Chen, Synthesis of MXene/DNA/Pd/Pt nanocomposite for sensitive detection of dopamine, *J. Electroanal. Chem.*, 2018, **816**, 189–194.

89 J. Zhao, C. He, W. Wu, H. Yang, L. Peng, L. Wen and Z. Hu, MXene-MoS_2 carbon-fiber-based flexible electrochemical interface for multiple bioanalysis in biofluids, *J. Chem. Eng.*, 2022, **446**, 136841.

90 Y. Dang, X. Guan, Y. Zhou, C. Hao, Y. Zhang, S. Chen, Y. Ma, Y. Bai, Y. Gong and Y. Gao, Biocompatible PB/Ti_3C_2 hybrid nanocomposites for the non-enzymatic electrochemical detection of H_2O_2 released from living cells, *Sens. Actuators, B*, 2020, **319**, 128259.

91 U. Amara, M. T. Mehran, B. Sarfaraz, K. Mahmood, A. Hayat, M. Nasir, S. Riaz and M. H. Nawaz, Perylene diimide/MXene-modified graphitic pencil electrode-based electrochemical sensor for dopamine detection, *Microchim. Acta*, 2021, **188**, 230.

92 W. Niamsi, N. Larpant, P. K. Kalambate, V. Primpray, C. Karuwan, N. Rodthongkum and W. Laiwattanapaisal, Paper-Based Screen-Printed Ionic-Liquid/Graphene Electrode Integrated with Prussian Blue/MXene Nanocomposites Enabled Electrochemical Detection for Glucose Sensing, *Biosensors*, 2022, **12**, 852.

93 D. Chen, S. Shao, W. Zhang, J. Zhao and M. Lian, Nitrogen and sulfur co-doping strategy to trigger the peroxidase-like and electrochemical activity of Ti_3C_2 nanosheets for sensitive uric acid detection, *Anal. Chim. Acta*, 2022, **1197**, 339520.

94 J. Chen, Y. Chen, S. Li, J. Yang, J. Dong and X. Lu, MXene/CNTs/Cu-MOF electrochemical probe for detecting tyrosine, *Carbon*, 2022, **199**, 110–118.

95 Y. Gogotsi and B. Anasori, The Rise of MXenes, *ACS Nano*, 2019, **13**, 8491–8494.

96 D. H. Ho, Y. Y. Choi, S. B. Jo, J. M. Myoung and J. H. Cho, Sensing with MXenes:Progress and Prospects, *Adv. Mater.*, 2021, **13**, 33.